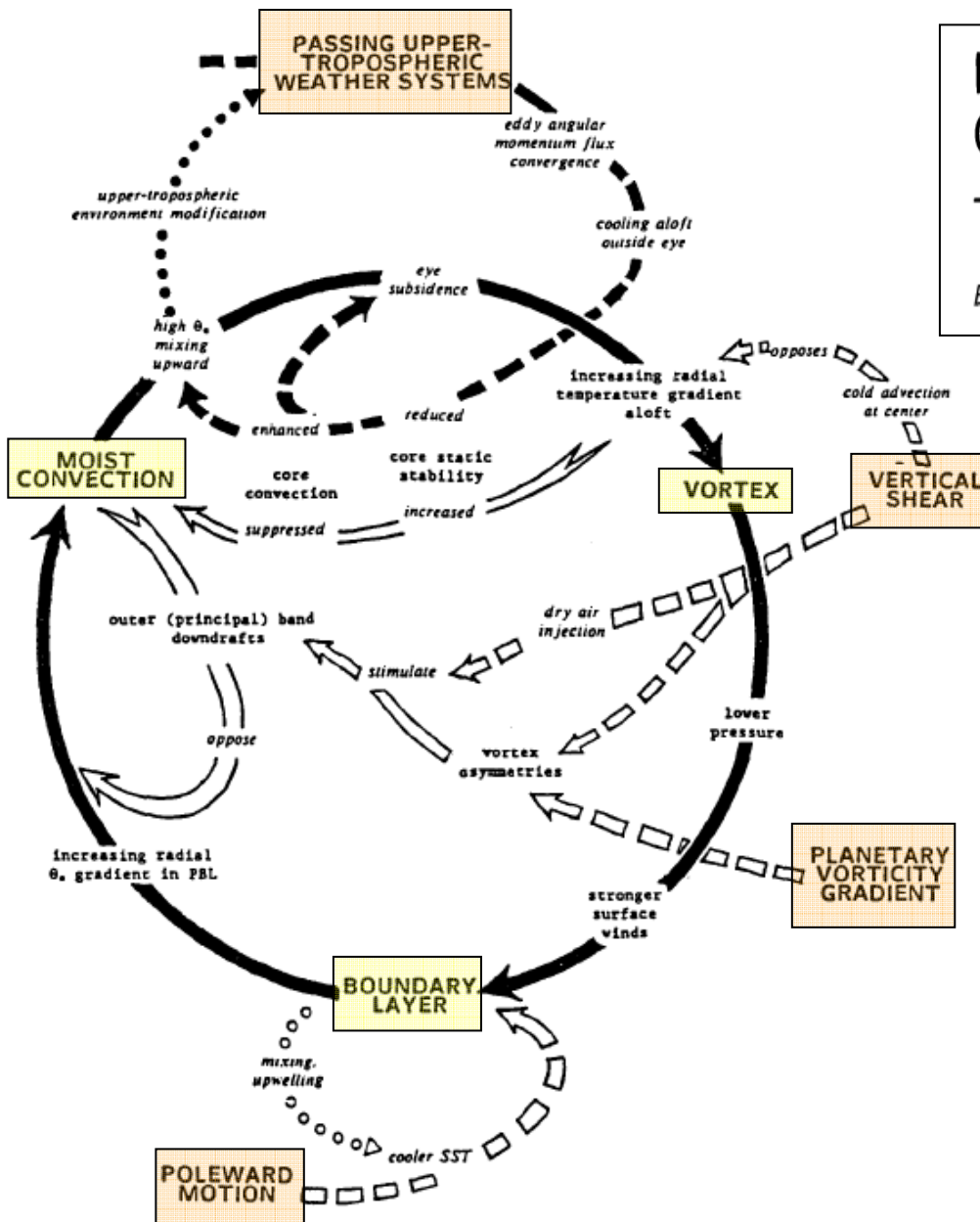


2. Influences externes

- Cisaillement de vent
- Air sec (saharien)
- Structures d'altitude
- Déplacement des cyclones
- Arrivée sur les terres
- Transition extra-tropicale
- Les risques

INFLUENCES EXTERNES



Is There Any Hope for Tropical Cyclone Intensity Prediction? —A Panel Discussion

Russell L. Elsberry*,
Greg J. Holland†,
Hal Gerrish‡,
Mark DeMaria‡,
Charles P. Guard***,
Kerry Emanuel***

Bulletin American Meteorological Society Vol. 73, No. 3, March 1992

Processes influencing tropical cyclone intensity change.

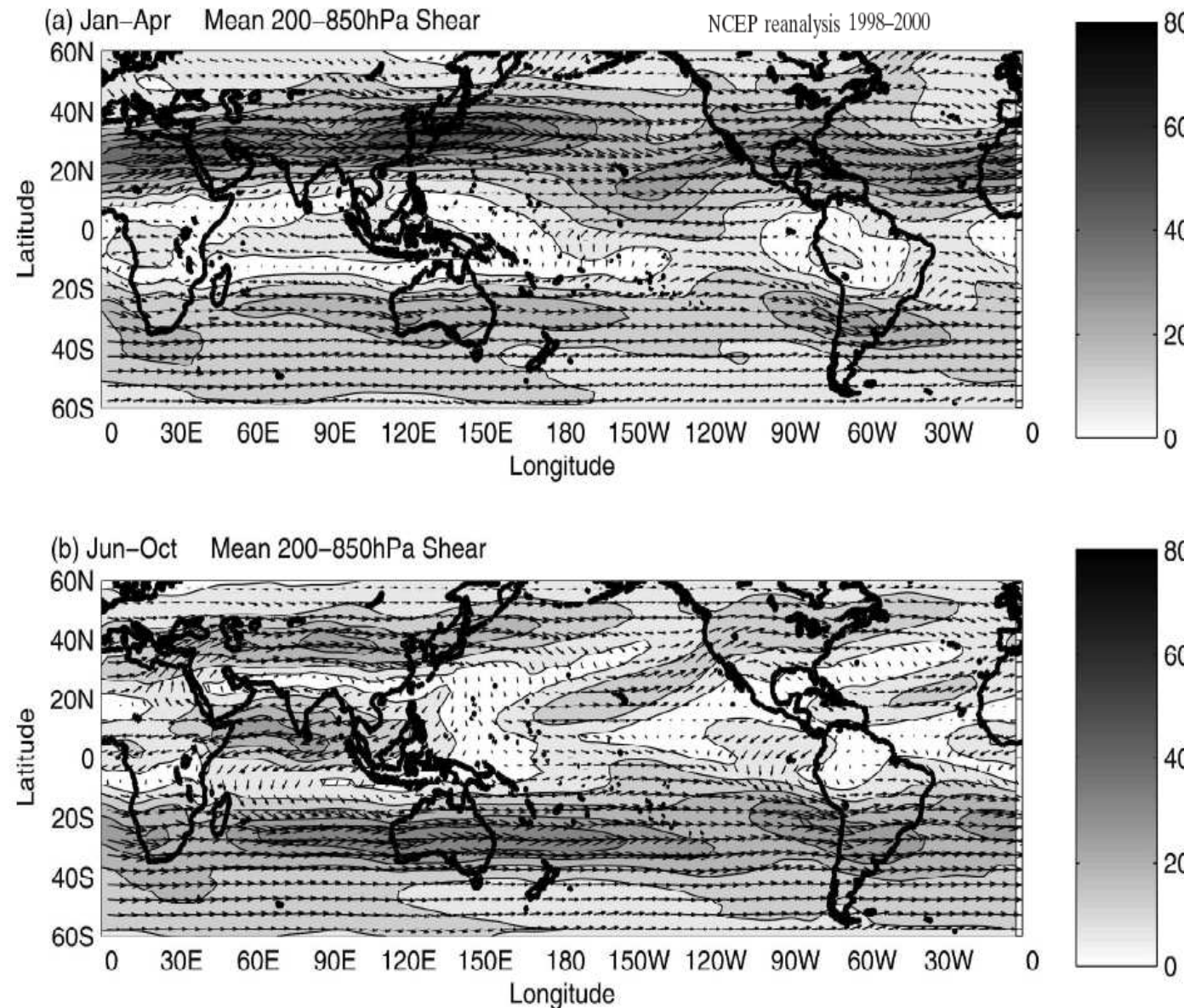
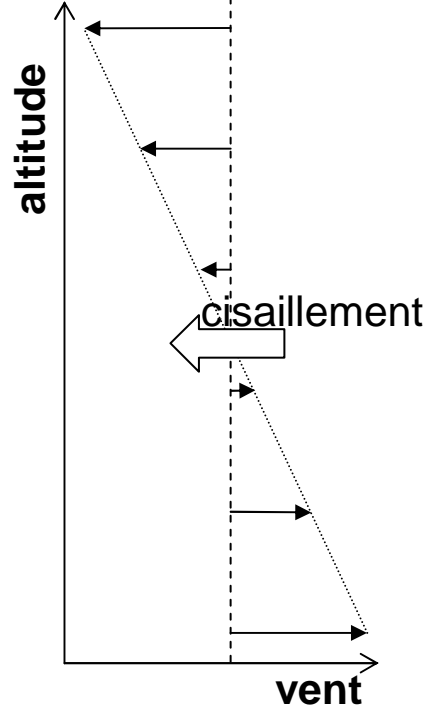
The black circle represents internal positive feedbacks between the vortex, the boundary layer, and moist convection.

Negative internal feedbacks are shown as white arrows.

Dashed arrows indicate positive (black)/negative (white) environmental influences

dotted arrows denote modification of the environment by the tropical cyclone

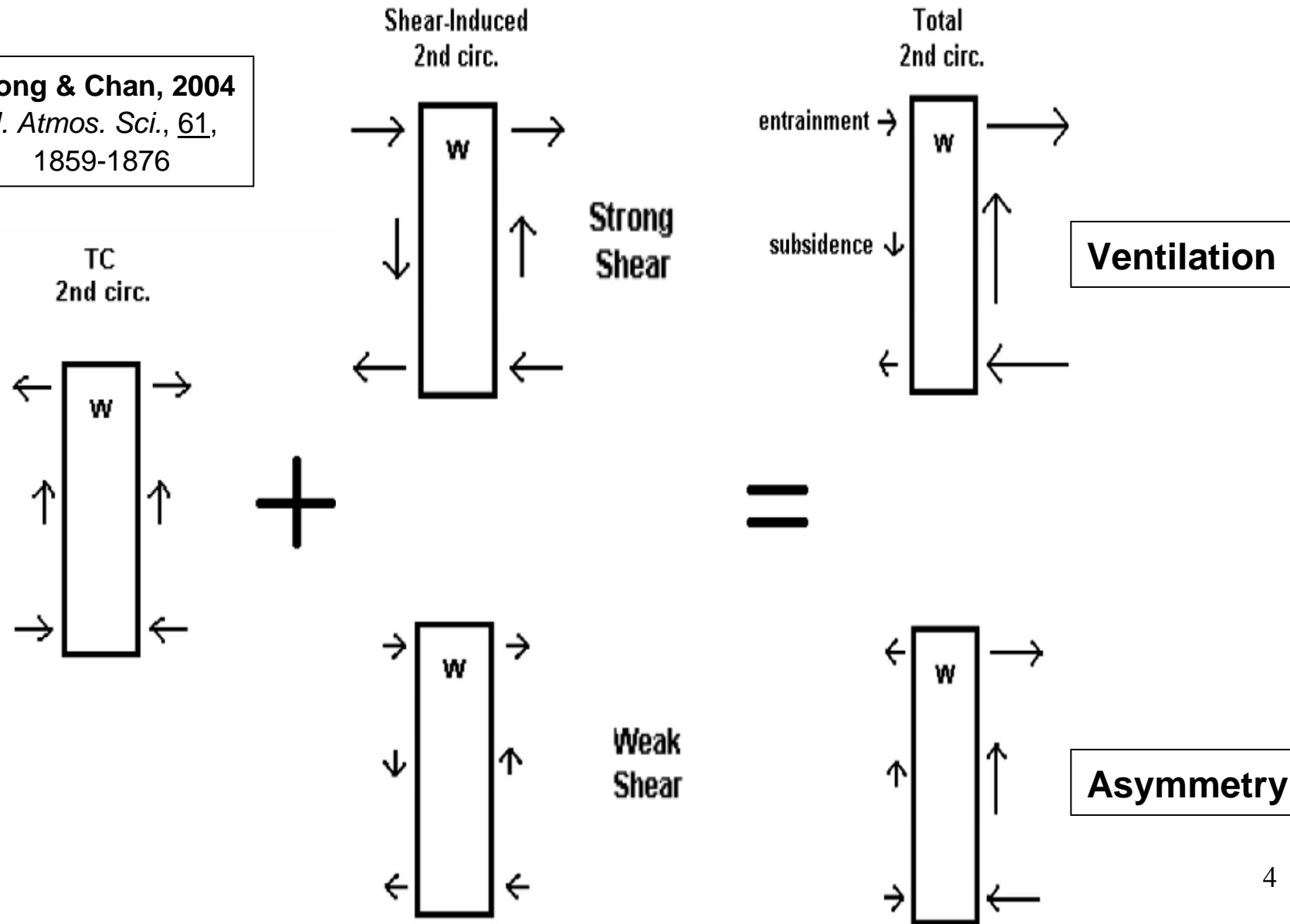
CISAILLEMENT DE VENT (1)



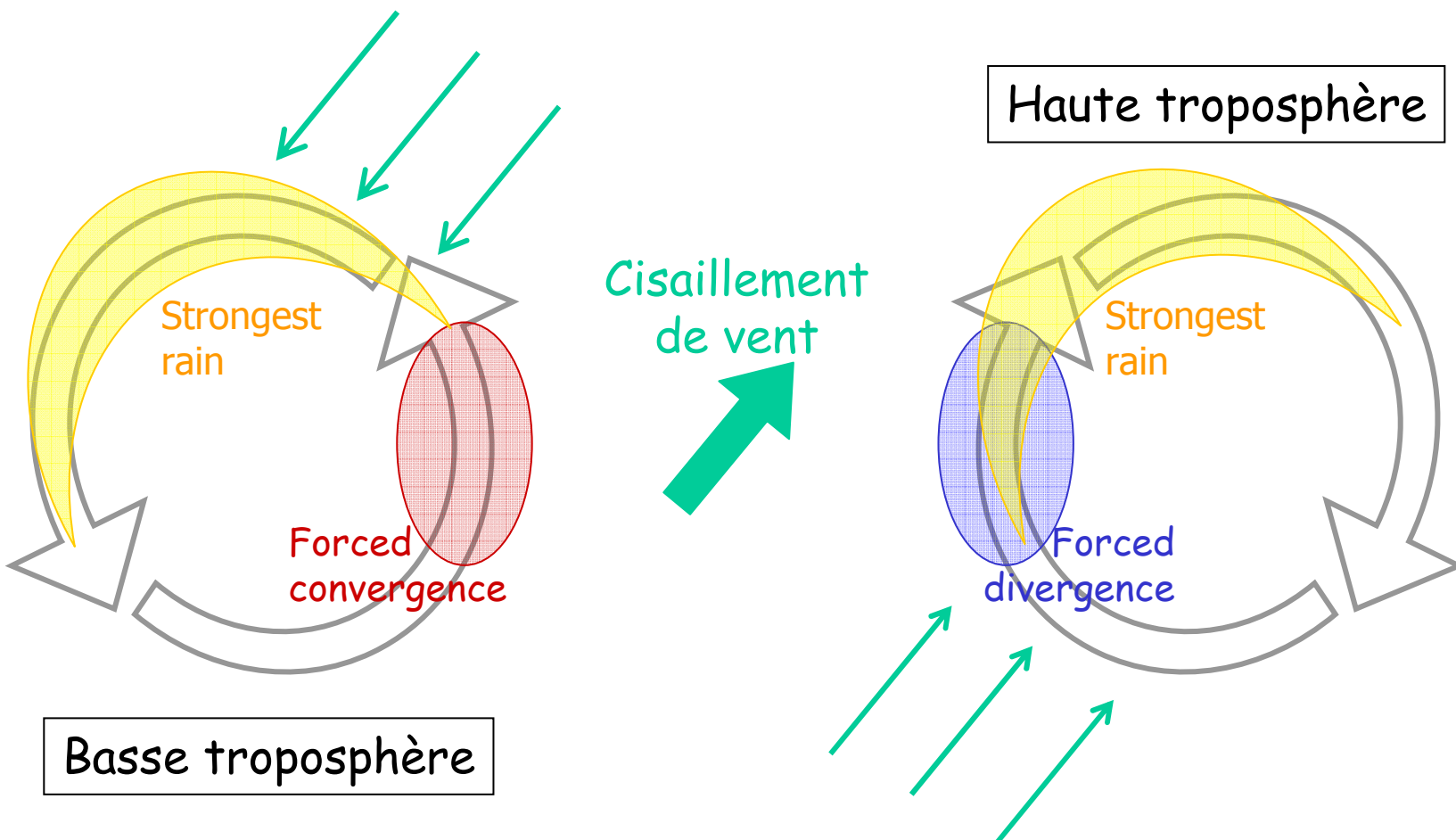
Chen et al. 2006,
Mon. Wea. Rev.,
134, 3190–3208

CISAILLEMENT DE VENT (2)

Wong & Chan, 2004
J. Atmos. Sci., 61,
1859-1876



CISAILLEMENT DE VENT (3)



CISAILLEMENT DE VENT (4)

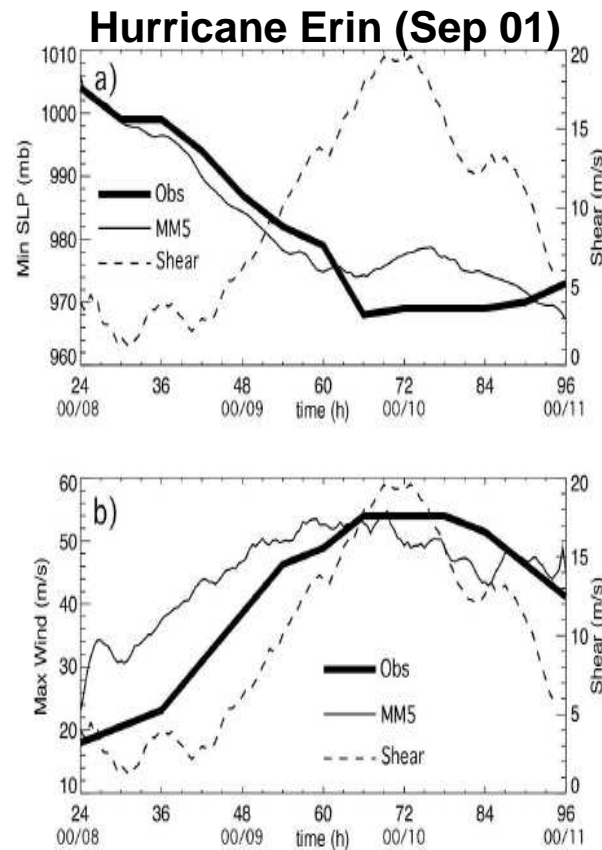


FIG. 3. Time series of simulated (thin solid line) and observed (thick line) (a) minimum sea level pressure and (b) maximum wind speed at the lowest model level. The dashed line shows the magnitude of the 850–200-mb vertical wind shear averaged over a circle of radius 300 km.

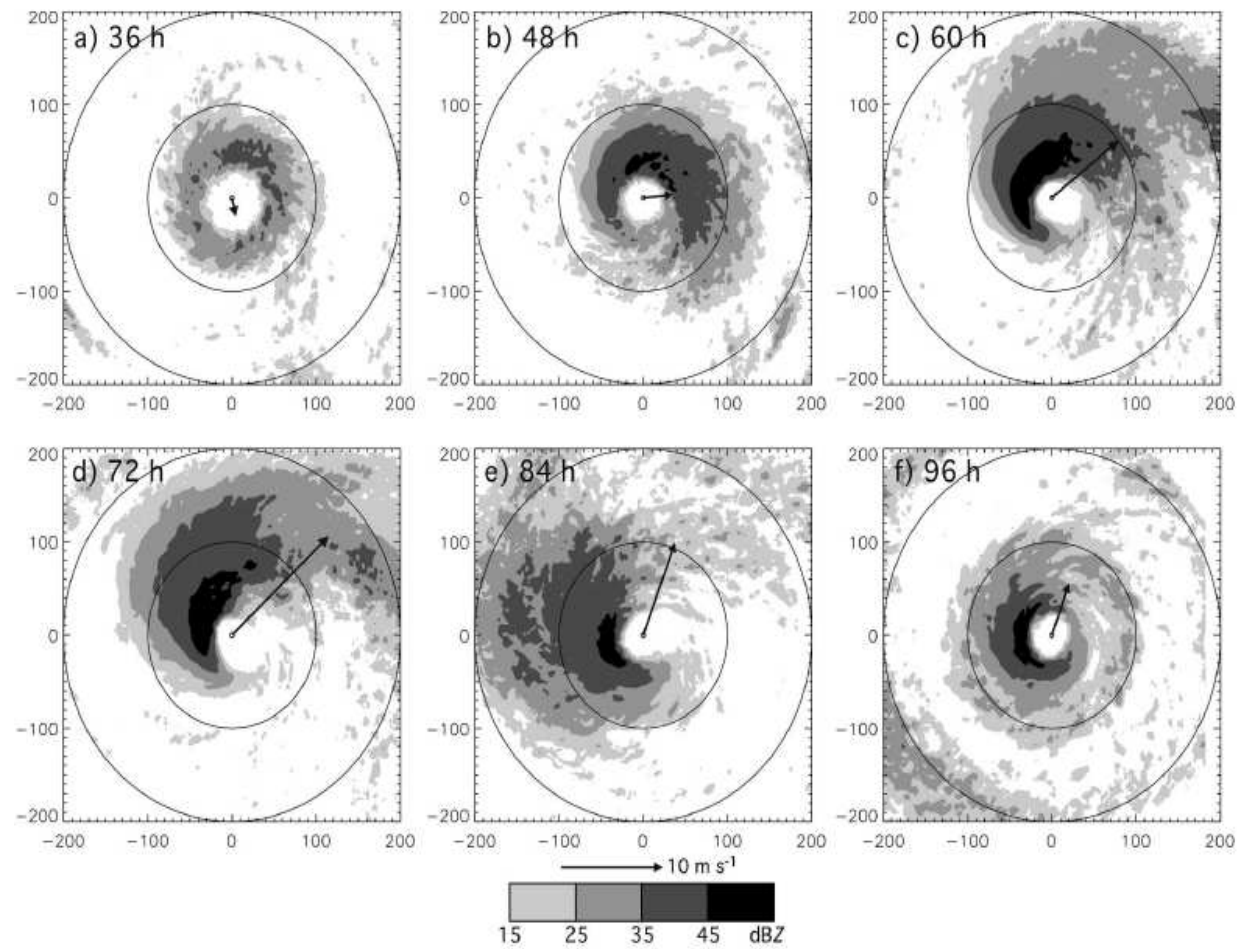


FIG. 5. Simulated radar reflectivity structure at the lowest model level (38 m). Contours show the simulated radar reflectivity averaged over the 6-h period ending at the indicated time. Arrows show the 6-h-averaged 850–200-mb vertical wind shear vector. Axis labels are in km with the origin at the storm center.

CISAILLEMENT DE VENT (5)

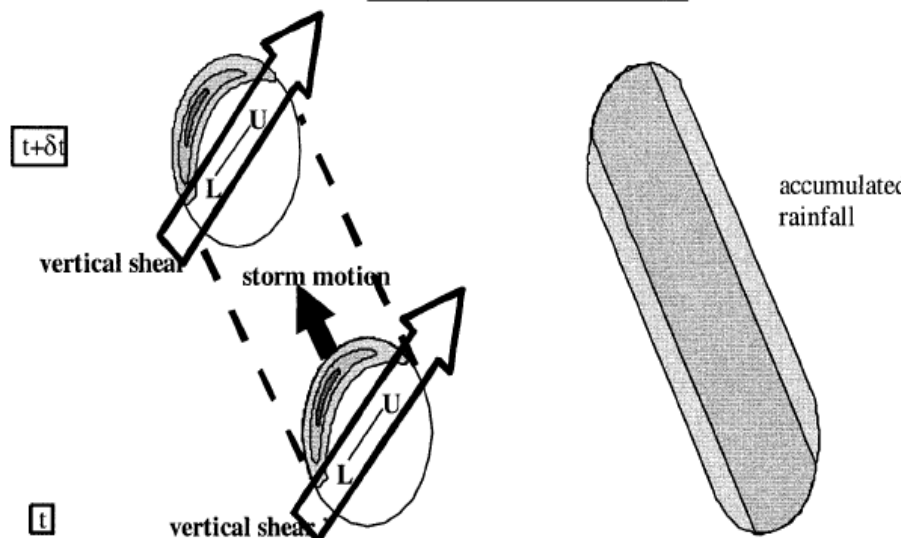
Rogers et al., 2003
Mon. Wea. Rev., 131, 1577-1599

The strongest convection in the core was generally located on the downshear left side of the shear vector when the shear was strong. the vortex showed a generally downshear tilt from the vertical.

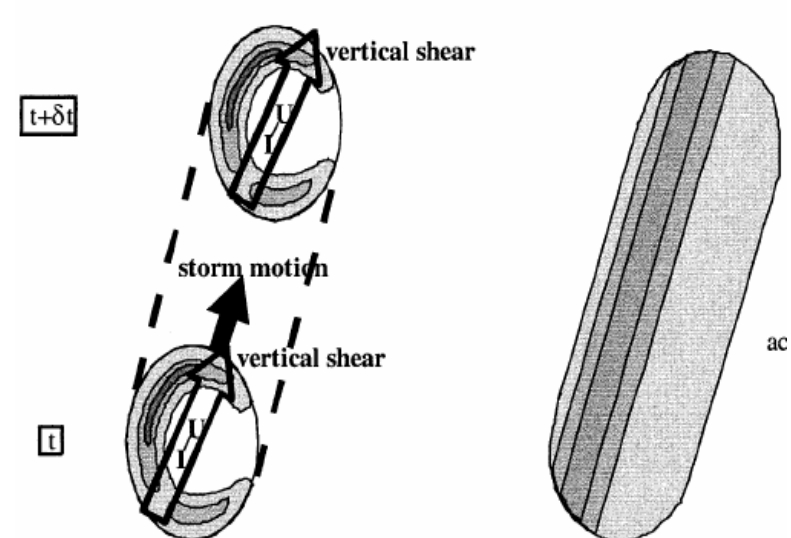
The magnitude of the tilt correlated well with changes in magnitude of the environmental shear.

The accumulated rainfall was distributed symmetrically across the track of the storm when the shear was strong and across track, and it was distributed asymmetrically across the track of the storm when the shear was weak and along track.

across-track shear



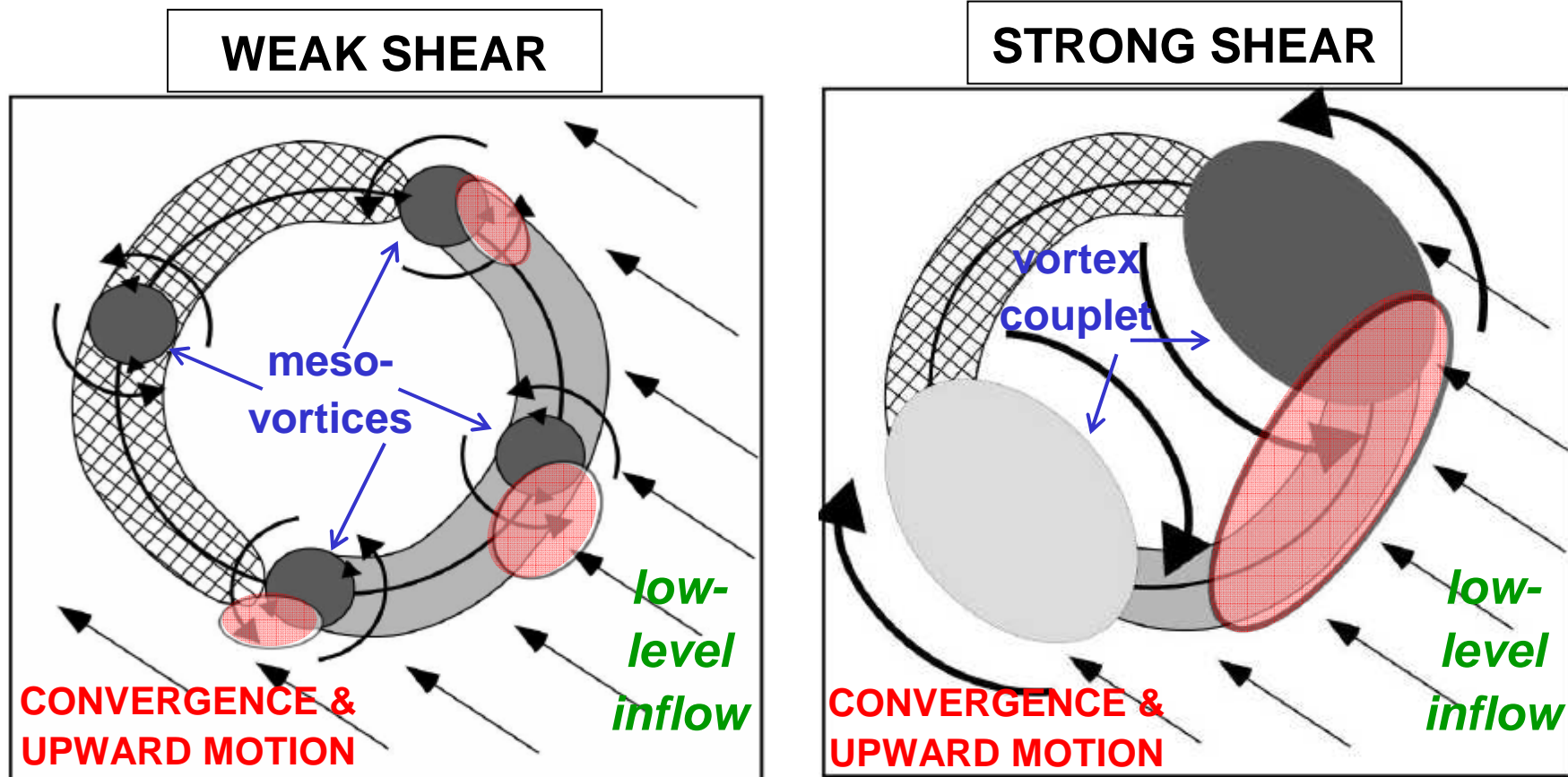
along-track shear



Simplified schematic showing relationships between shear, storm heading, vortex tilt, instantaneous rainfall (reflectivity), and total rainfall.

Shading in left column denotes reflectivity (i.e., rain rates).
Shading in right column denotes total accumulated rainfall during δt .
Symbols L and U in left column denote locations of lower- and upper-level vortex centers, respectively.

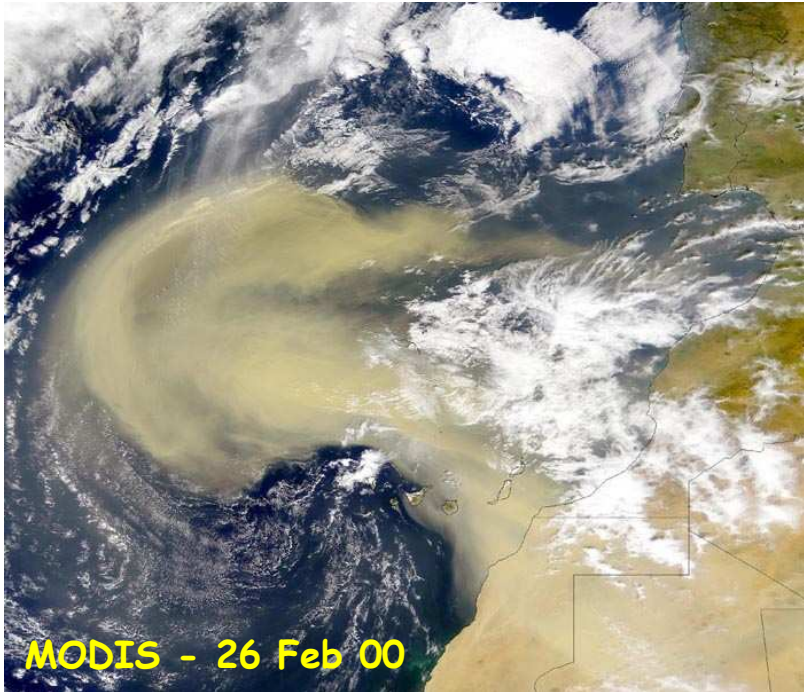
CISAILLEMENT DE VENT (6)



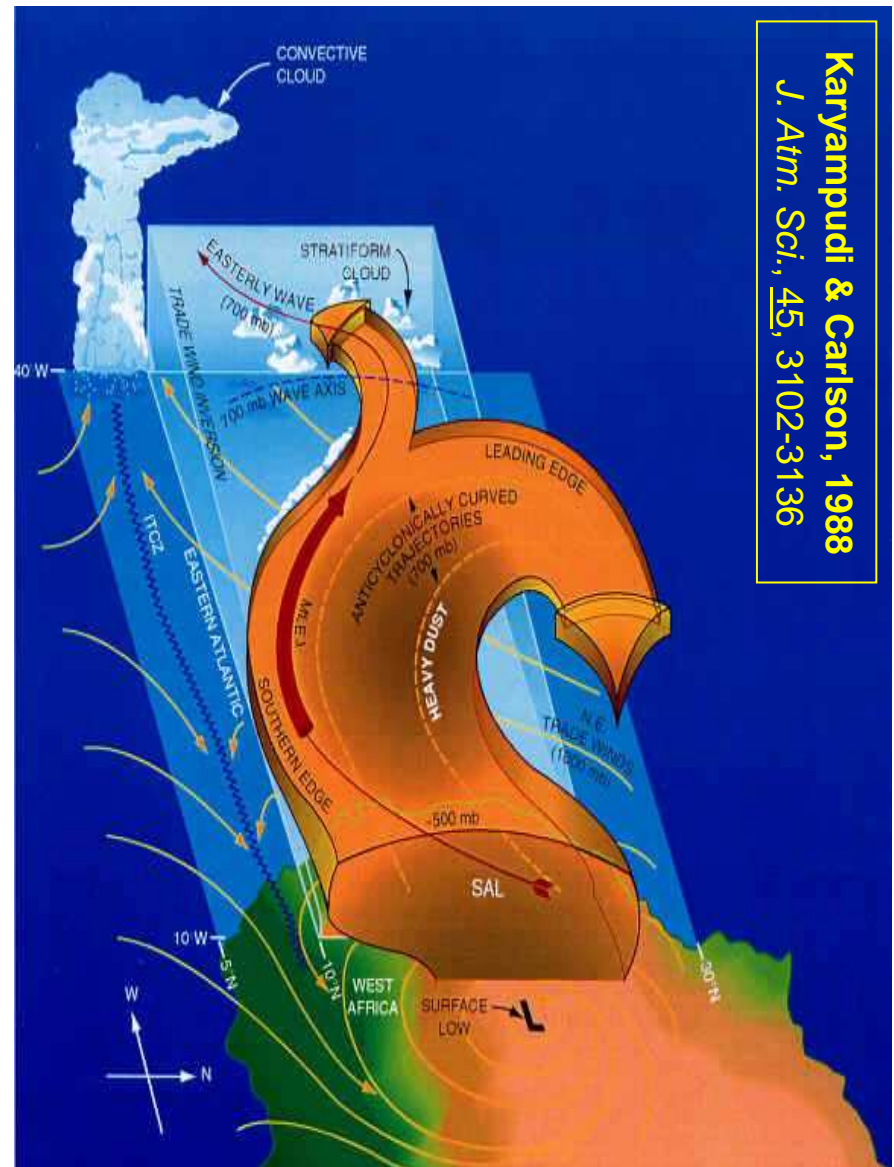
Eyewall mesovortices are associated with convective-scale updrafts. They move around the eyewall at a speed slower than the maximum tangential wind

The eyewall is dominated by a cyclonic-anticyclonic vortex couplet producing a strong flow across the eye which converges with the low-level inflow and induces a strong asymmetric updraft.⁸

AIR SEC (SAHARIEN)



De larges zones d'air très sec (Hum. Rel. <50%) et chargé en aérosols émanent parfois du Sahara et se propagent sur l'Atlantique tropical. Ces masses d'air s'étendent entre 1500 et 6000 m et elles sont associées à des vents forts (10-25 ms⁻¹) en moyenne troposphère.



Karyampudi & Carlson, 1988
J. Atm. Sci., 45, 3102-3136

Impact sur les cyclones :

- Inversion de basses couches $\Delta T_{SAL} \approx 5-10^\circ C$
- Intrusion d'air très sec à 850-600 hPa
- Renforcement du cisaillement de vent
(Jet d'Est Africain renforcé vers 700 hPa)
- Influence des aérosols sur la microphysique ?

- Propagation sur de grandes distances, sans modification majeure des caractéristiques
- Détection difficile en dehors des images satellites

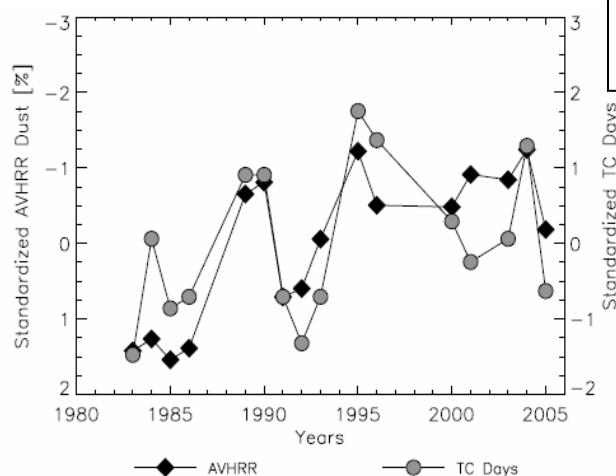
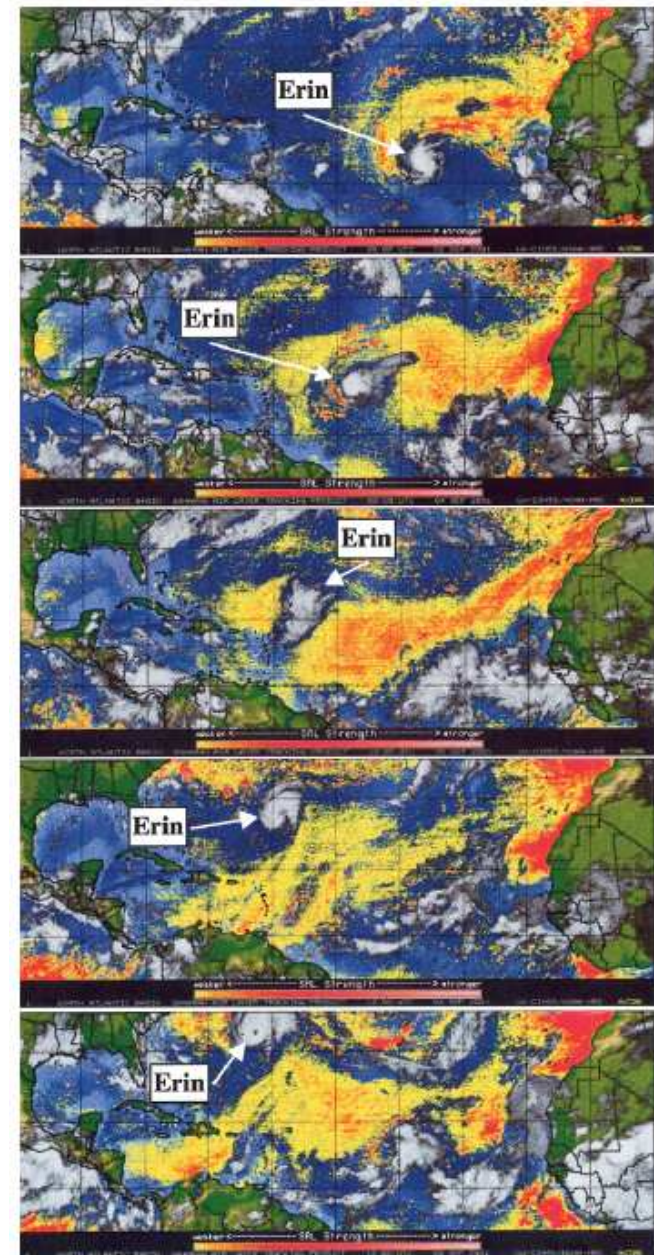


Figure 4. Same description as Figure 3 except that data points from three positive phase (1982, 1987 and 1997), and two negative phase (1998 and 1999) ENSO events, and a year with missing satellite data (1984) are removed. The correlation coefficient between the two time series is 0.71, significant at the 99.9% level.

Dunion & Velden, 2004

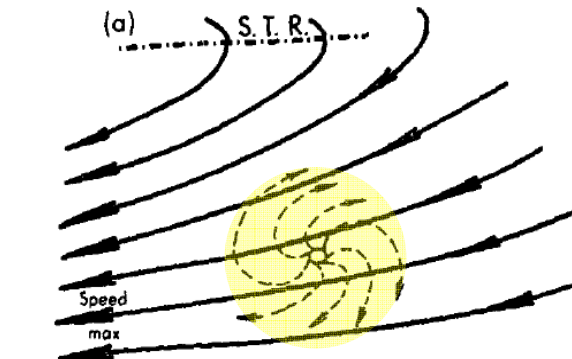
Bull. Amer. Meteor. Soc., 84, 353-365



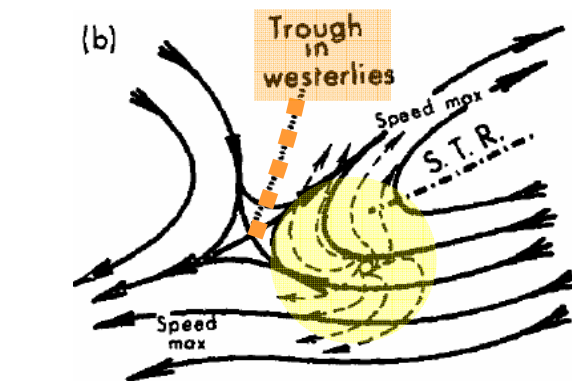
STRUCTURES D'ALTITUDE (1)

Sadler, 1976

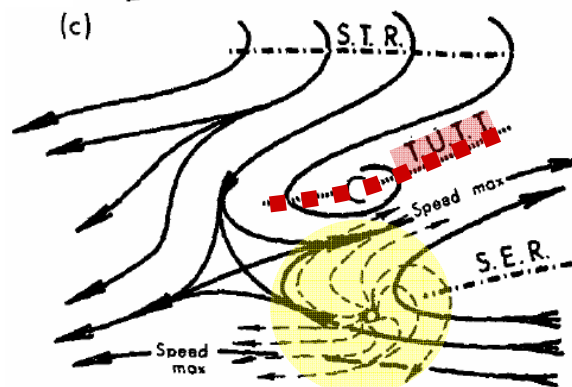
Mon. Wea. Rev., 104, 1266-1278



Flux de nord-est en altitude (S de Dorsale SubTrop) → blocage de la circulation divergente anticyclonique au nord + renforcement du cisaillement : Conditions défavorables



Automne : Thalweg de la circulation d'ouest des moyennes latitudes → partie est permet l'évacuation de la circulation divergente anticyclonique au nord : Conditions favorables

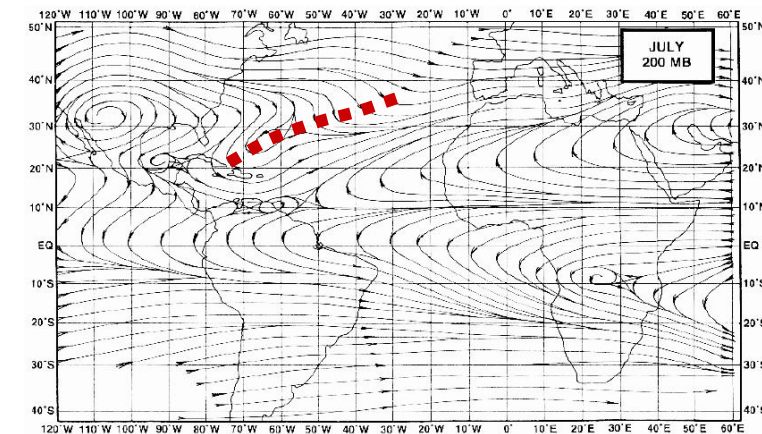
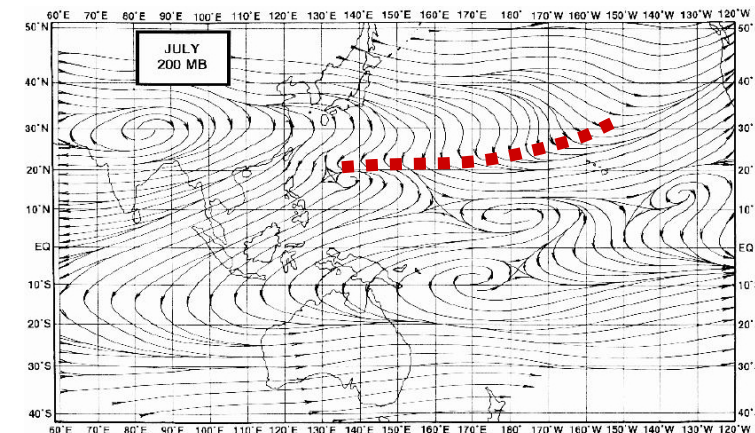
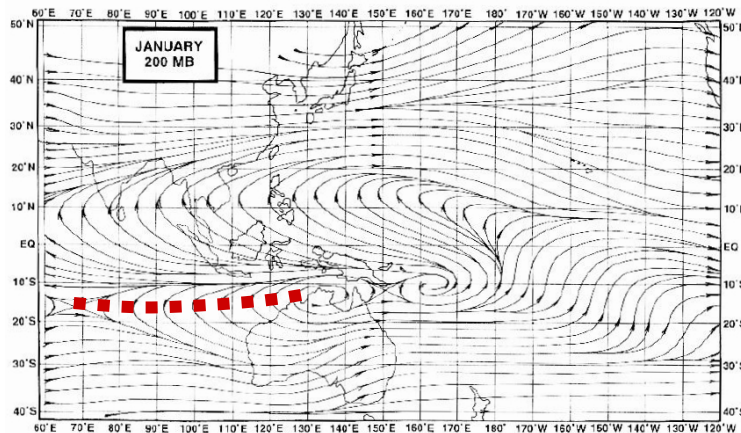


Eté : « Tropical Upper Tropospheric Trough » → partie est permet l'évacuation de la circulation divergente anticyclonique au nord : Conditions favorables

STRUCTURES D'ALTITUDE (2)

Tropical Upper Tropospheric Trough - TUTT

Thalweg de Haute Troposphère Tropicale - THTT : phénomène « climatologique » de grande dimension, orienté NNE-SSW, fréquent en été sur le Pacifique (sud et nord) et l'Atlantique nord



« TUTT cells » : partie non stationnaire de l'écoulement TUTT

STRUCTURES D'ALTITUDE (3)

Hanley et al., 2001
Mon. Wea. Rev., 129, 2570-2584

Interactions THTT - cyclone

Facteurs favorables :

- canal d'évacuation du flux divergent d'altitude,
- renforcement du tourbillon cyclonique par la convergence du flux associé de moment angulaire.

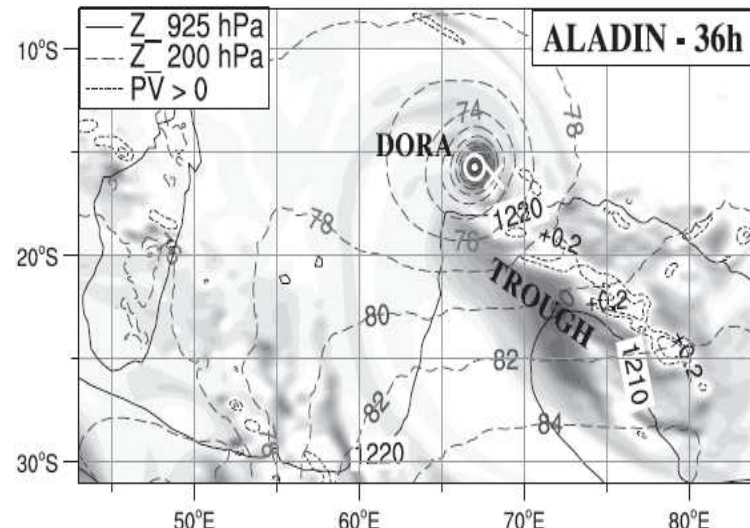
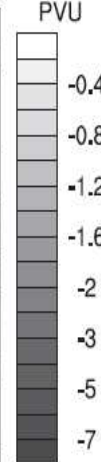
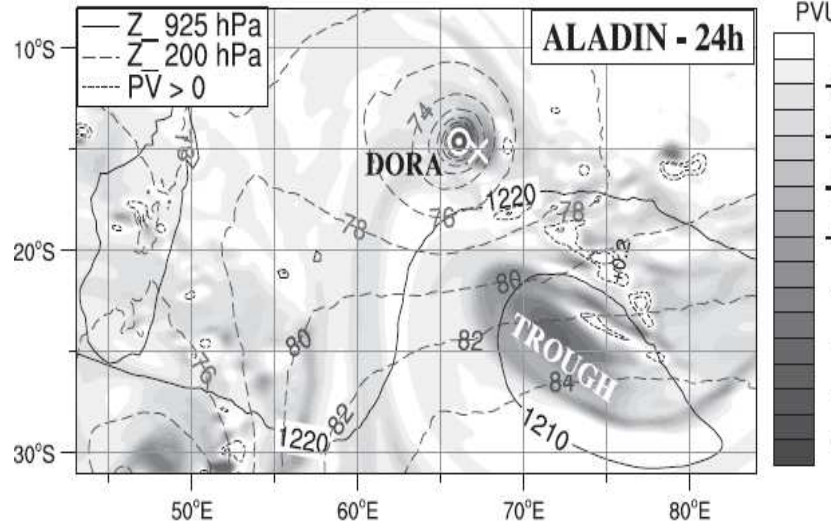
Facteur défavorable :

- augmentation du cisaillement de vent.

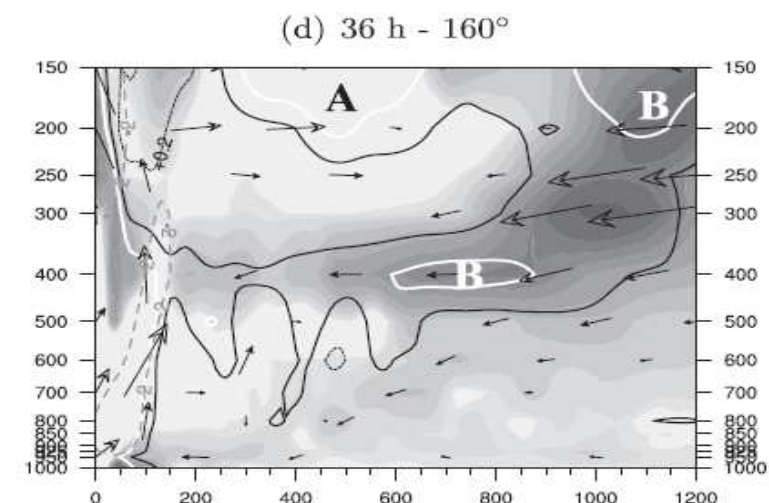
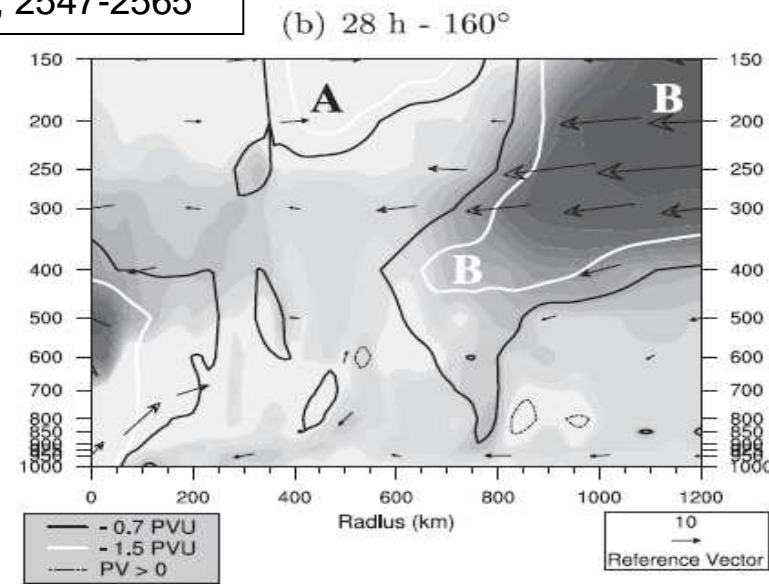
Pas de conclusion définitive (sensibilité aux analyses ...)

STRUCTURES D'ALTITUDE (4)

Leroux et al., 2013
J. Atmos. Sci., 70, 2547-2565

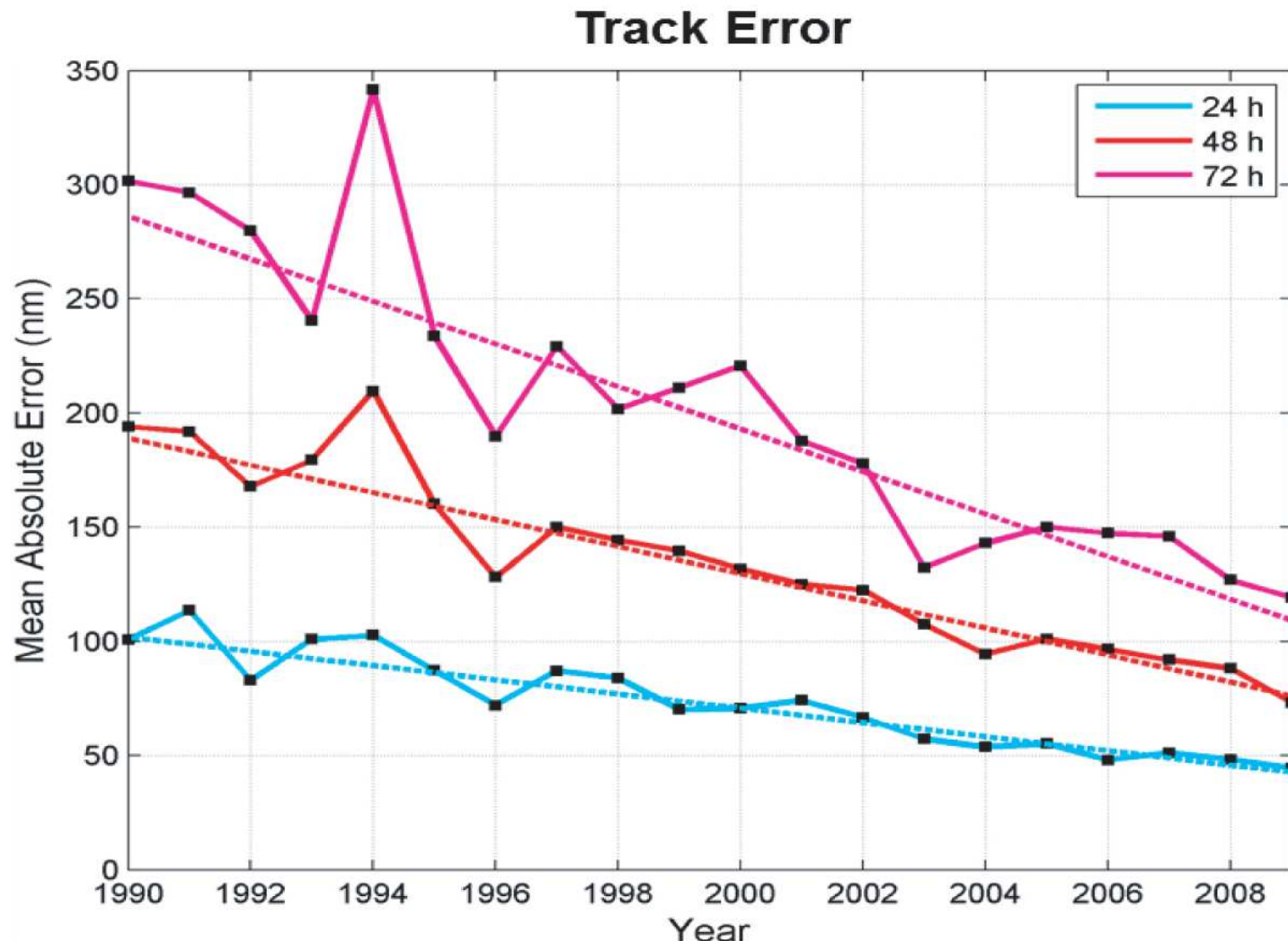


Aladin-Reunion forecast for TC Dora
 from 0600 UTC 31 Jan 2007



Radius-pressure cross sections
 of PV radial advection

LE DEPLACEMENT DES CYCLONES (1)



Average mean absolute errors for official TC track predictions at various lead times in the North Atlantic basin from 1990-2009.

[National Hurricane Center, Miami, FL, USA]

LE DEPLACEMENT DES CYCLONES (2)

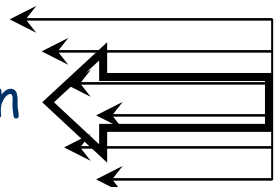
Chan, 2005 : «The Physics of Tropical Cyclone Motion»
Ann. Rev. Fluid Mech., 37, 99-128

- Environnement barotrope ($\partial_h T$, $\partial_z V_H = 0$) :
 - Advection par le flux moyen
 - Effet β (gradient méridien du tourbillon planétaire)
 - Gradients horizontaux de tourbillon relatif
- Environnement barocline ($\partial_h T$, $\partial_z V_H \neq 0$) :
 - Basses (moyennes) latitudes : vers la droite (gauche) du cisaillement
 - Décalage vers les maximums de $\partial_t PV$
 - Advection due à la dynamique interne & externe
 - Libération de chaleur latente

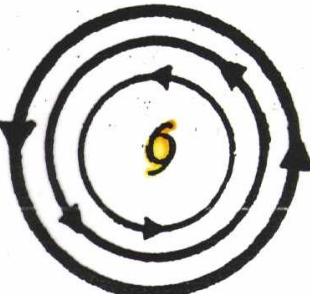
LE DEPLACEMENT DES CYCLONES (3)

Plusieurs composantes interviennent simultanément:

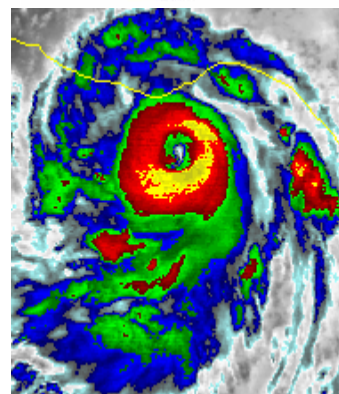
- le vent moyen



- le tourbillon moyen



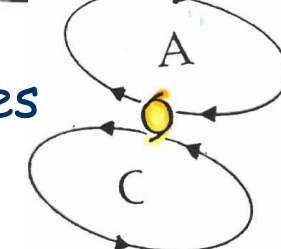
- la convection dans le Mur de l 'Œil et dans les bandes externes



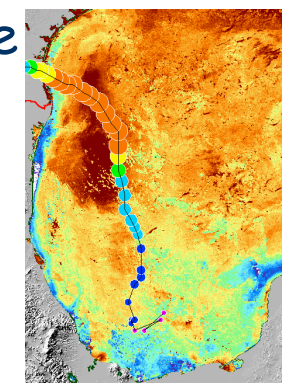
- les perturbations proches



- les tourbillons internes (ordre 1 + ...)



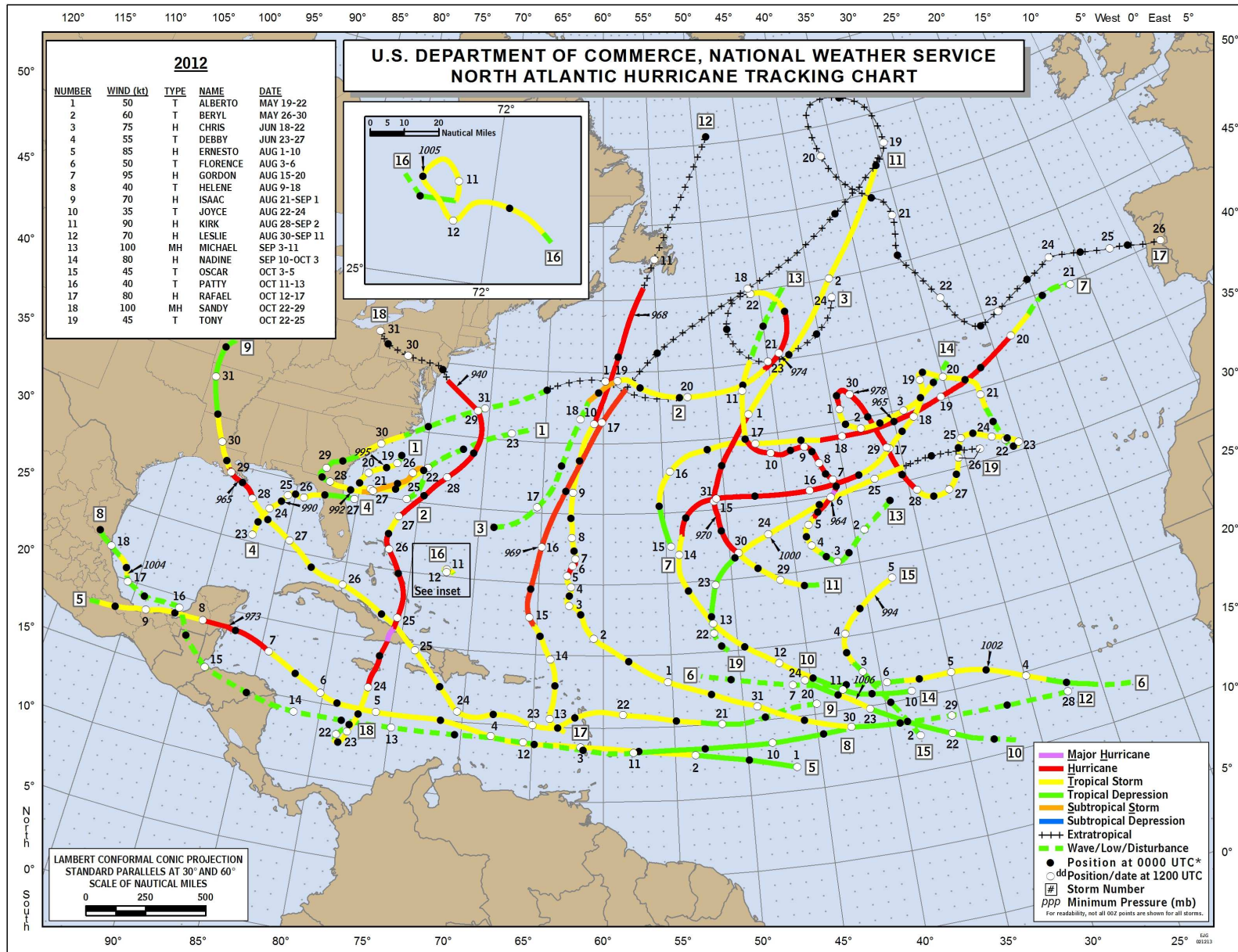
- la température de surface océanique



- le relief

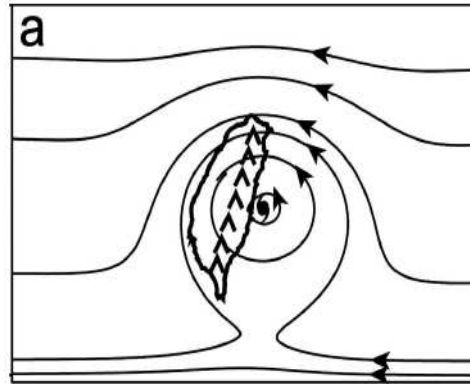
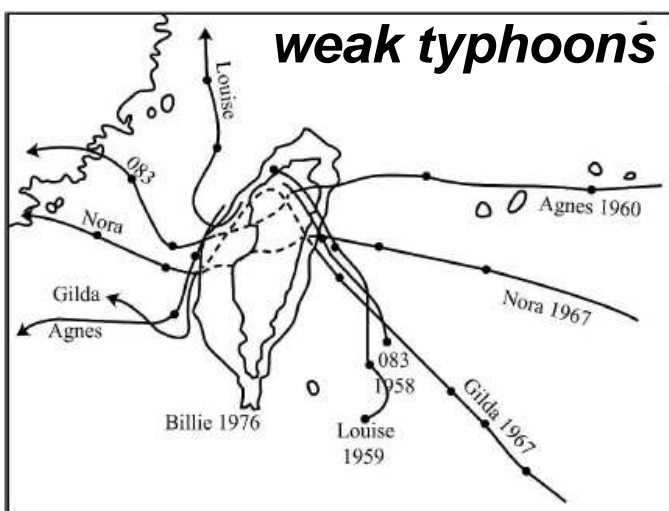
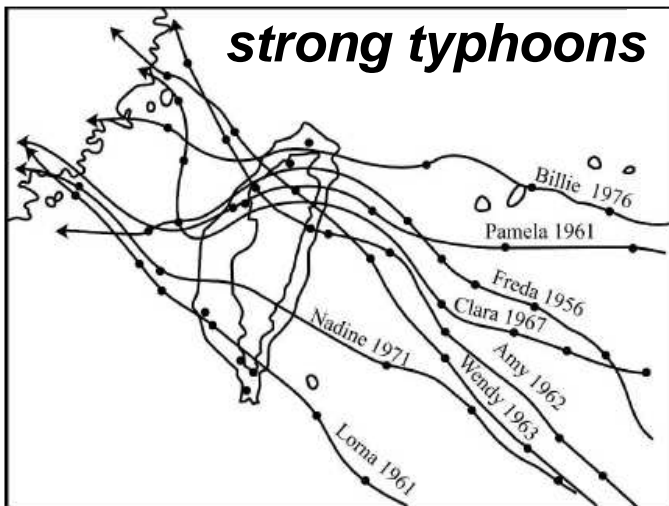


LE DEPLACEMENT DES CYCLONES (ex: 2012)

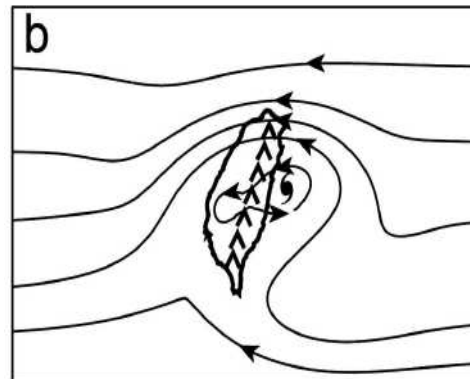


LE DEPLACEMENT DES CYCLONES (4)

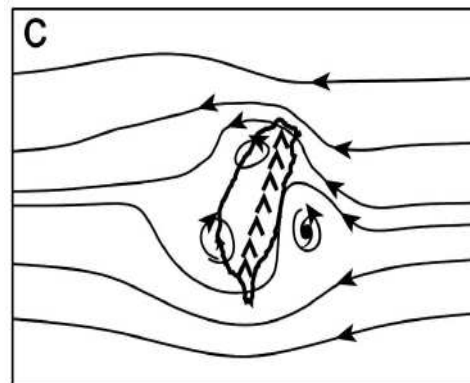
Lin et al., 2006
Mon. Wea. Rev., 134, 3509-3538



Weak blocking : *northward upstream, then southward downstream deflection, continuous track.*



Moderate blocking : *northward upstream deflection, secondary vortex on the lee side, discontinuous track.*

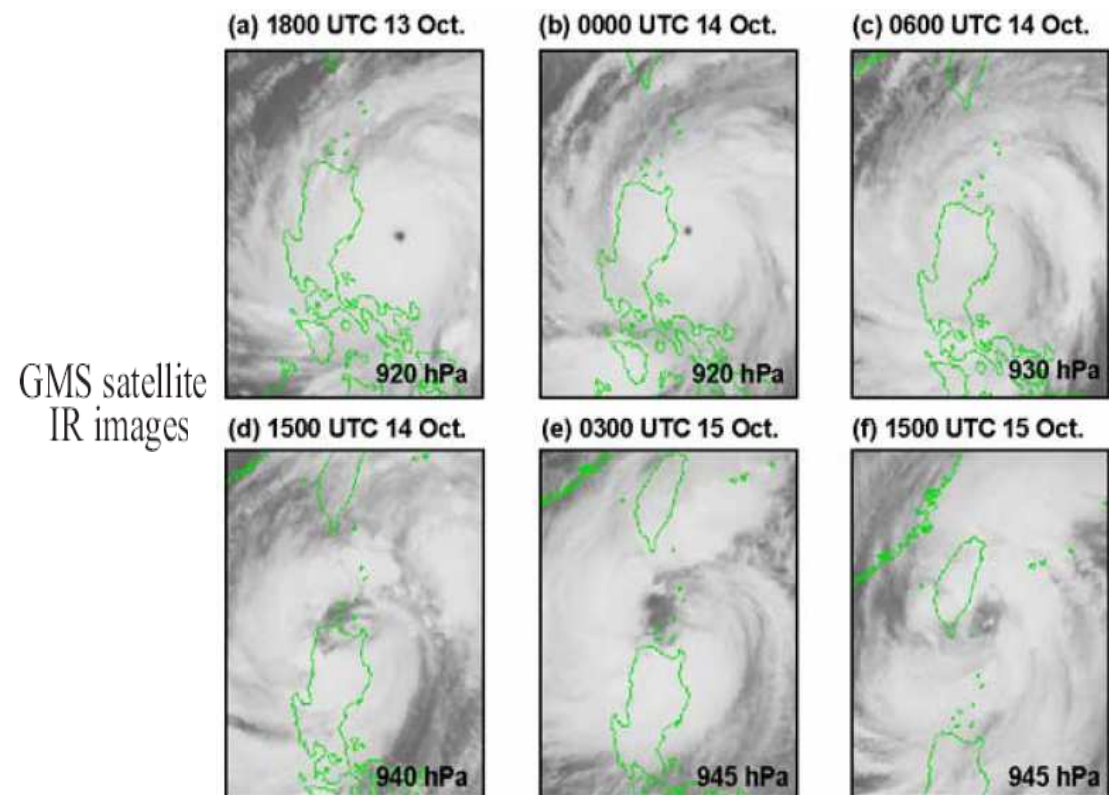
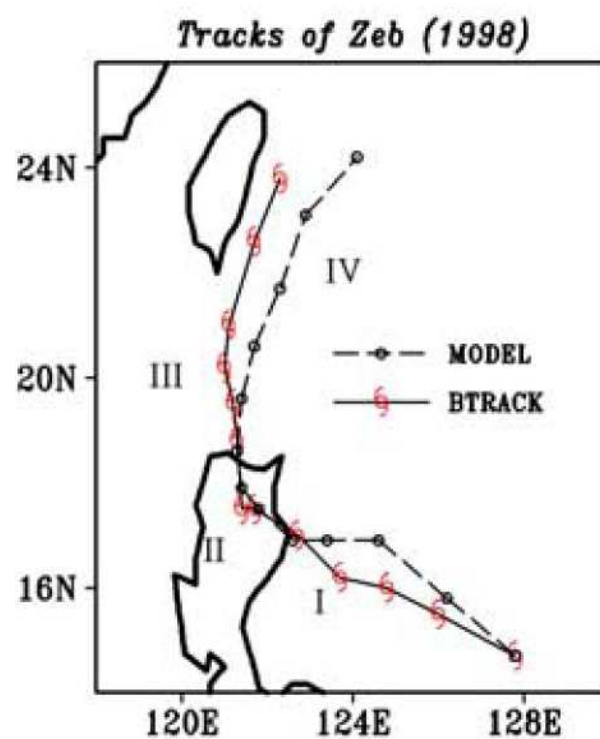


Strong blocking : *southward upstream deflection, secondary vortices on the lee side, discontinuous track.*

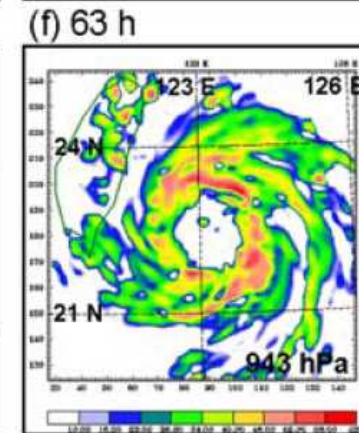
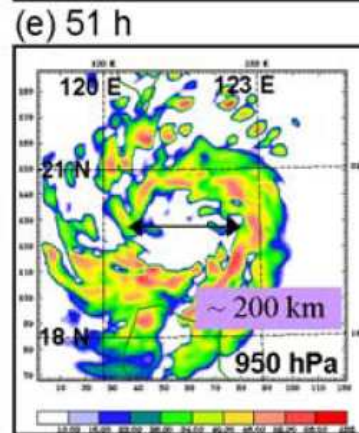
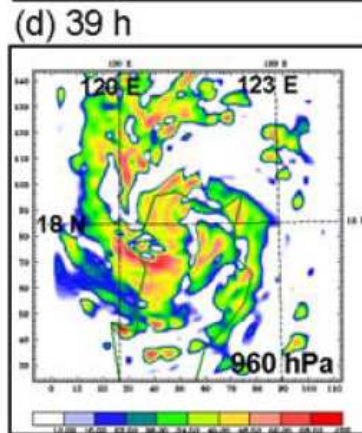
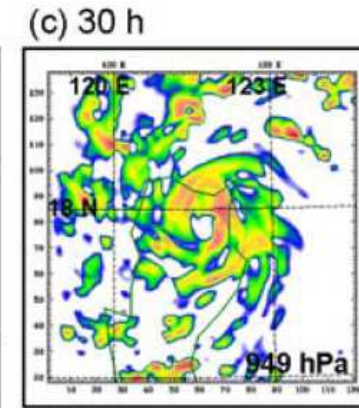
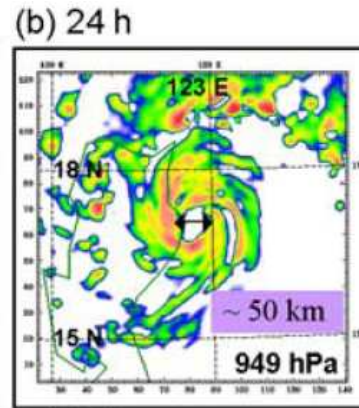
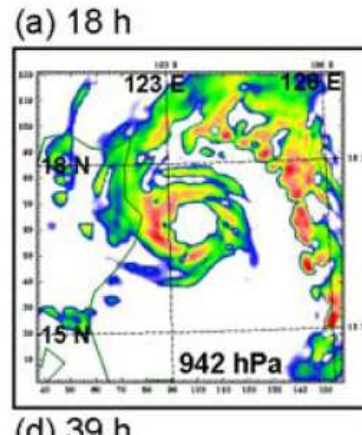
ARRIVEE SUR LES TERRES (1)

Wu et al. 2003 [*Geophys. Res. Lett.*, 30, 6.1-4]

- Evolution of typhoon Zeb (1998) before, during and after its landfall at Luzon documented with satellite observations and MM5 (45 / 15 / 5 km, 72 h simulation starting 00 UTC 13 Oct 98, 24 h prior to landfall)
- The terrain plays a critical role in leading the observed evolution : first eyewall contraction just before landfall, a following breakdown, the eyewall reformation after the storm returned to the ocean

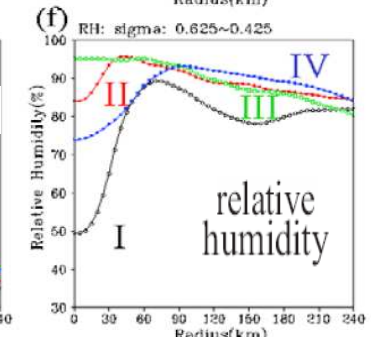
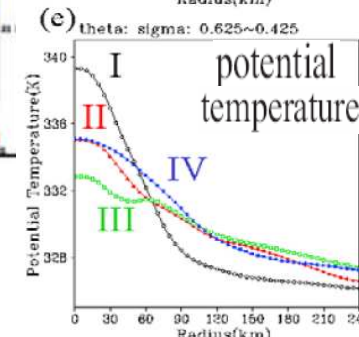
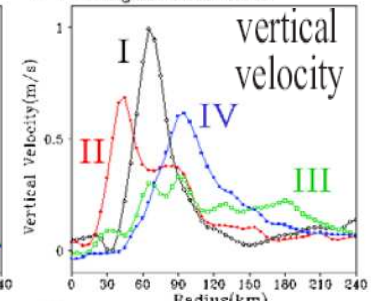
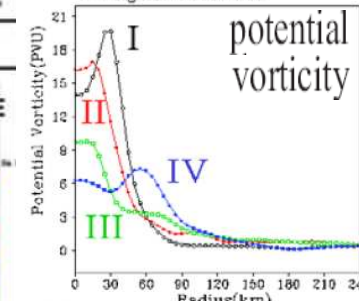
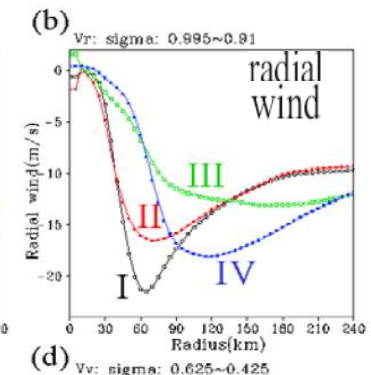
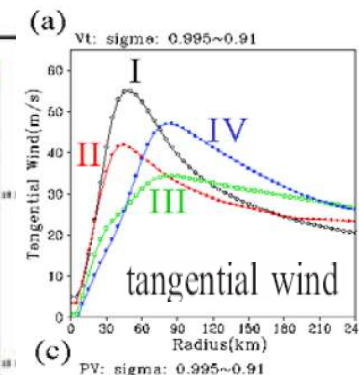


ARRIVEE SUR LES TERRES (2)



model-simulated radar reflectivity (dBZ) at 700 hPa

- (i) What are the key parameters determining the evolutionary processes of a landfalling TC?
- (ii) How does the eddy (the asymmetric component) interact with the mean flow (the symmetric component)?
- (iii) What kind of roles do the terrain, surface drag, and ocean heat flux play relative to those eyewall processes?

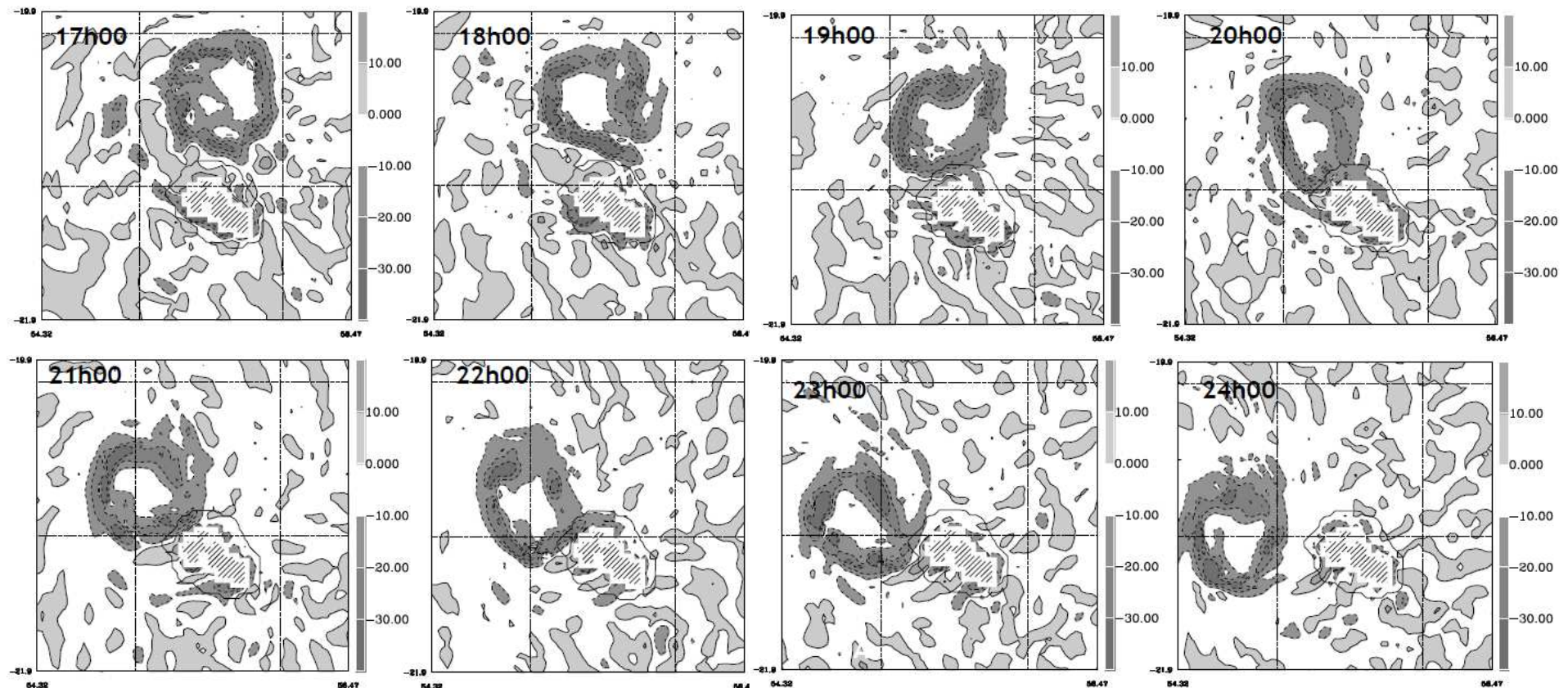


Time, azimuthal and vertical average

I : before landfall , II : landfall begins ,
III : inland , IV : return to the ocean

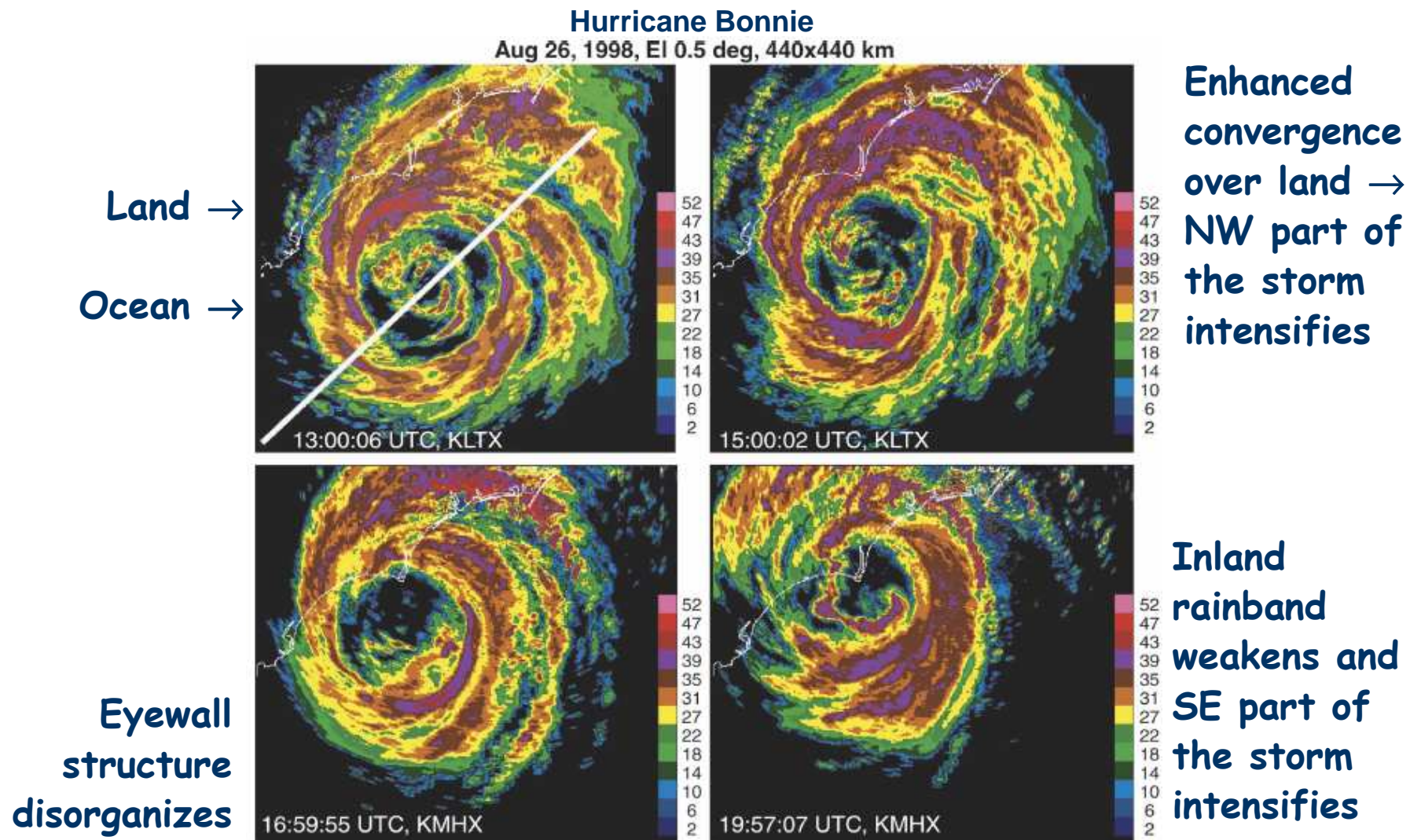
ARRIVEE SUR LES TERRES (3)

Jolivet *et al.* 2013 [*Ann. Geophys.*, 31, 107-125]
« A numerical study of orographic forcing on TC Dina (2002) in SW Indian ocean »



ARRIVEE SUR LES TERRES (4)

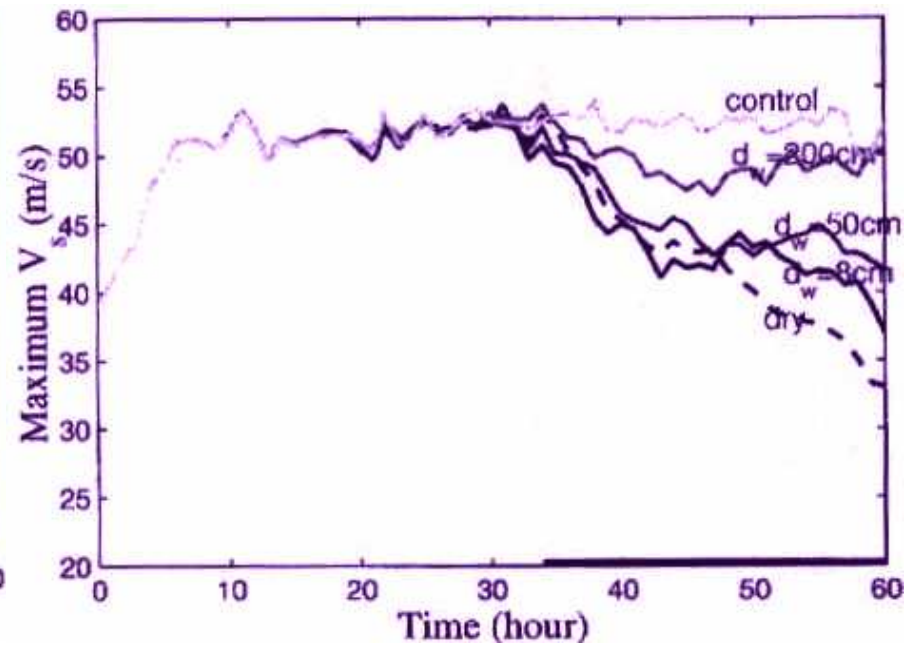
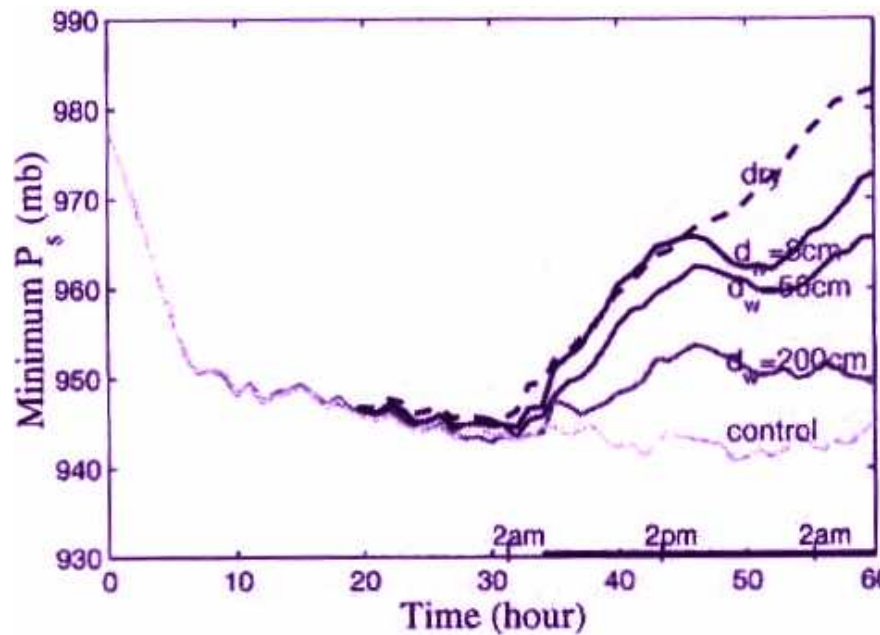
Schneider & Barnes, 2005
Mon. Wea. Rev., 133, 3243-3259



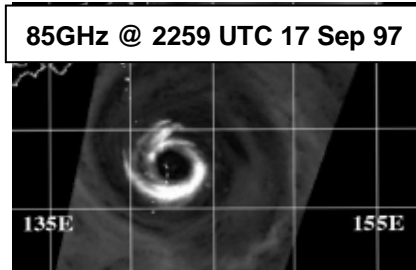
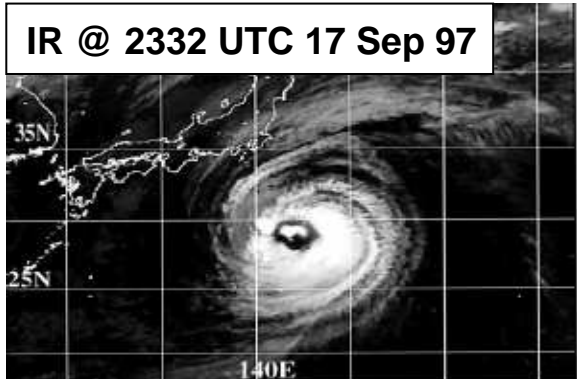
ARRIVEE SUR LES TERRES (5)

Shen et al. 2002 [*J. Atmos. Sci.*, 59, 789-802]

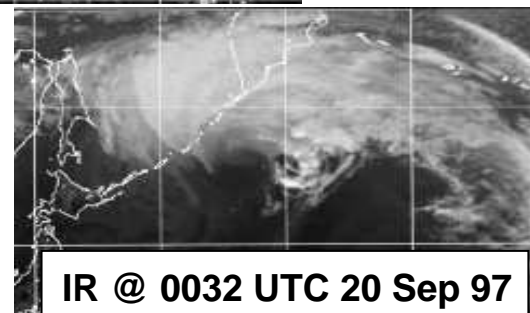
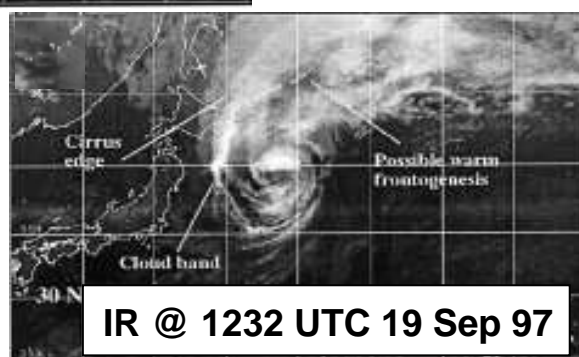
- little is known on the effect of surface water over land during decay of a landfalling tropical cyclone.
- Different water depths and surface conditions are considered [GFDL model, 1° / $1/3^\circ$ / $1/6^\circ$]
- a layer of 0.5 m water can noticeably reduce landfall decay
- increase of surface roughness reduces the surface winds, but barely change the surface temperature and evaporation patterns.



TRANSITION EXTRA-TROPICALE (1)

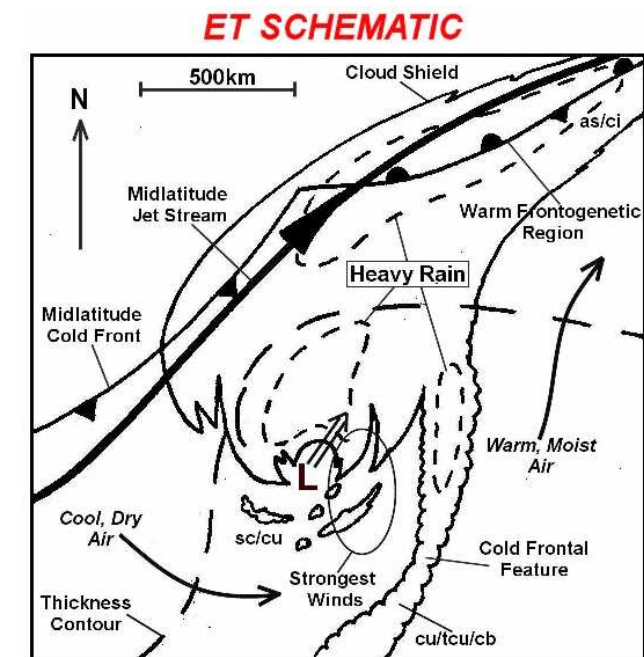
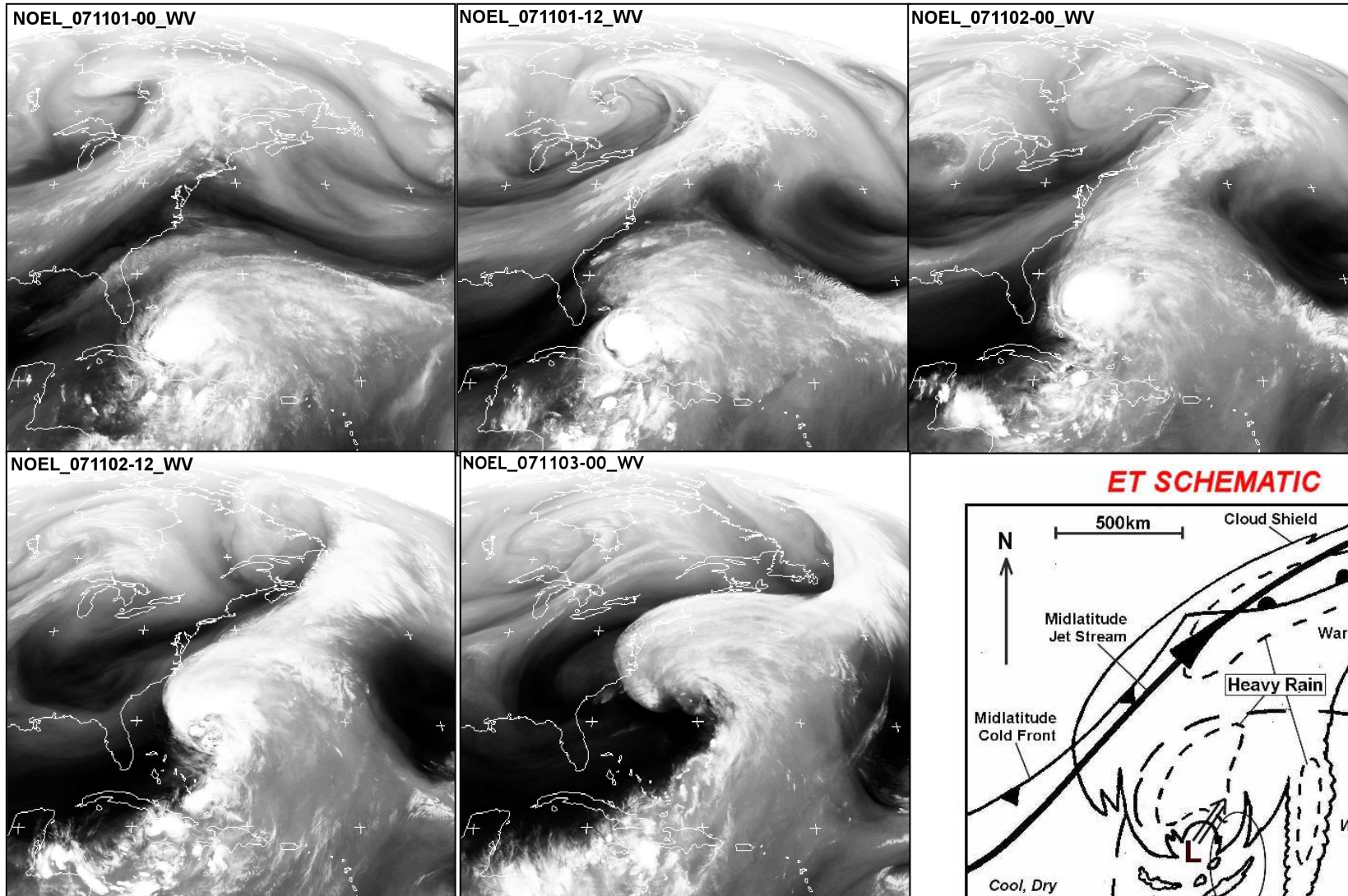


Klein et al., 2000
Wea. Forecasting, 15, 374-395

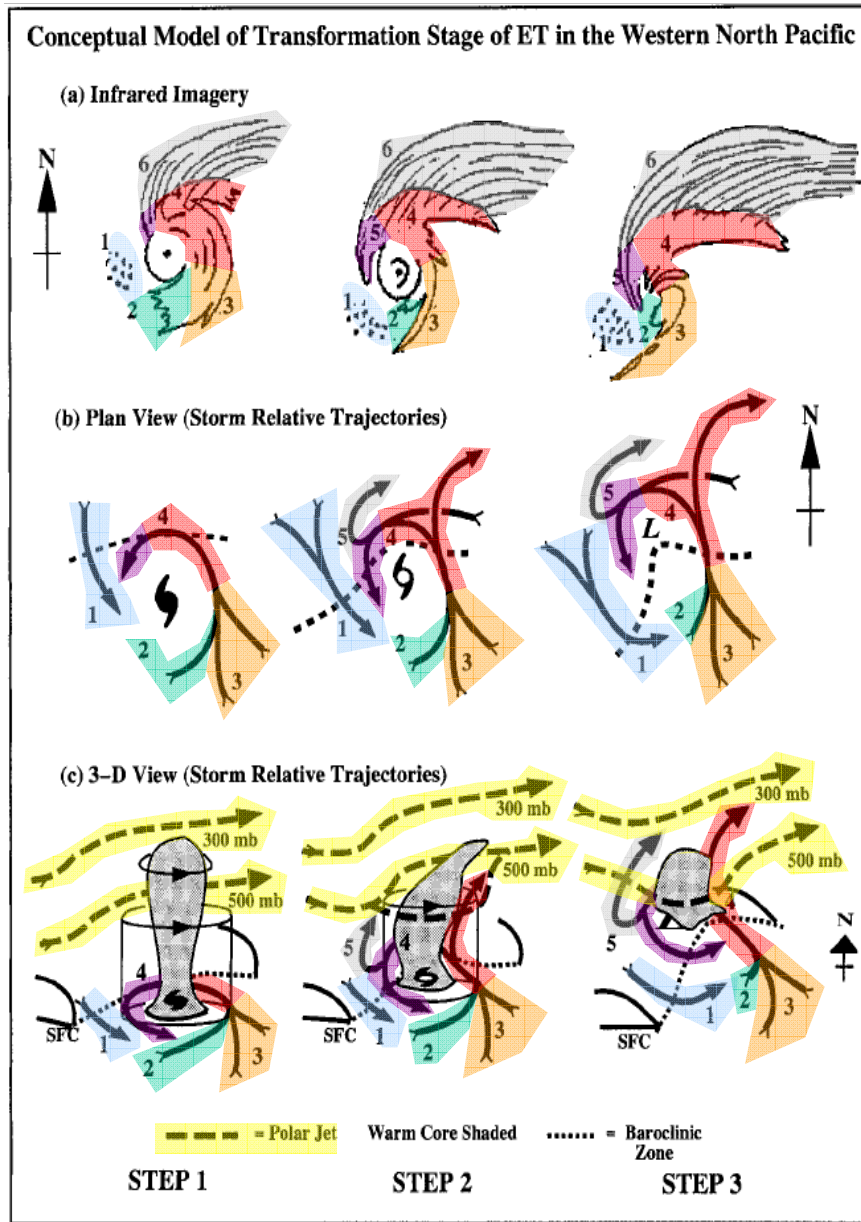


Typhon David (1987)

TRANSITION EXTRA-TROPICALE (2)



TRANSITION EXTRA-TROPICALE (3)



1. environmental equatorward flow of cooler, drier air with associated cell cumulus ;
2. decreased tropical cyclone convection in the western quadrant (with corresponding « dry slot » in STEP 1, which extends throughout the southern quadrant in STEPS 2 and 3) ;
3. environmental poleward flow of warm, moist air is ingested into tropical cyclone circulation, which maintains convection in the eastern quadrant and results in an asymmetric distribution of cloud and precipitation ;
4. ascent of warm, moist inflow over tilted isentropic surfaces associated with baroclinic zone (dashed line in the middle and lower panels) ;
5. ascent (undercut by dry-adiabatic descent) that produces cloudbands wrapping westward and equatorward around the storm center ; dry-adiabatic descent occurs close enough to the circulation center to produce erosion of eyewall convection in STEP 3
6. cirrus shielded with a sharp cloud edge if confluent with polar jet.

TRANSITION EXTRA-TROPICALE (4)

Agusti-Paneda *et al.*, 2004
Quart. J. Roy. Meteor. Soc., 130, 1047-1074

Figure 1. Schematic showing potential vorticity (PV) anomalies and other anomalies featuring in the extra-tropical transition process: (1) a surface thermal anomaly on a baroclinic zone, (2) diabatically-generated positive PV anomalies along the baroclinic zone, (3) a positive PV anomaly associated with a midlatitude upper-level trough, (4) the tropical-cyclone's positive PV anomaly and (5) the negative PV anomaly associated with the tropical-cyclone's outflow. The arrow represents an upper-level jet. The strength of the jet is associated with the horizontal gradient of PV at upper-levels, i.e. the steepness of the tropopause.

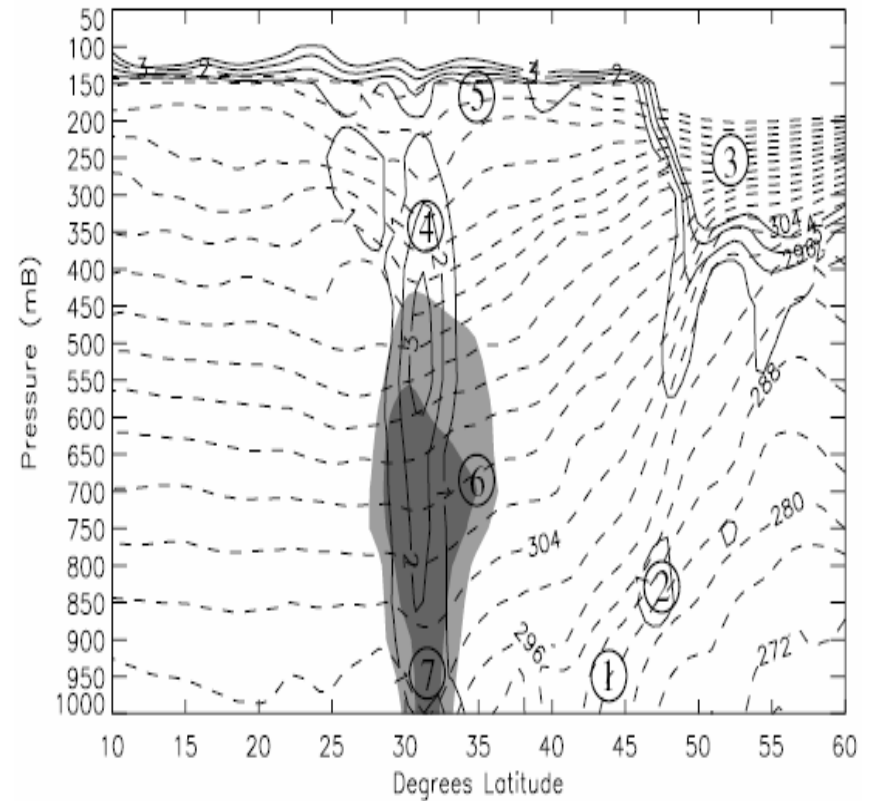
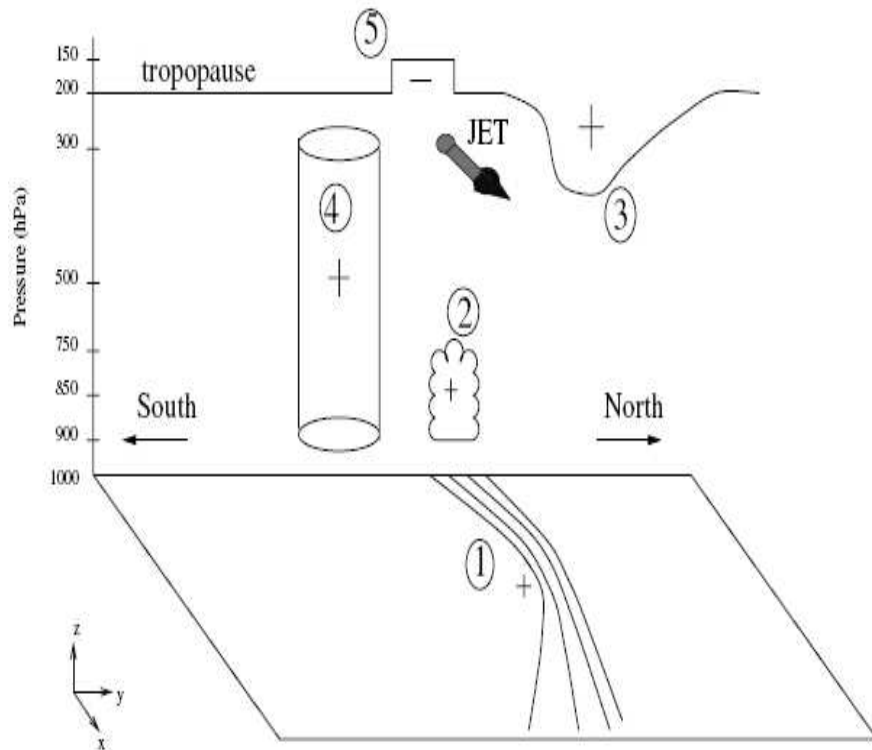


Figure 3. Potential vorticity (PV) and other anomalies involved in the extratropical transition of hurricane *Irene* (12 UTC 17 October 1999) shown by a north-south vertical cross-section of PV (full contours of 1, 2, 3 and 4 PVU), potential temperature from 272 K to 356 K (dashed contours with 4 K interval) and mixing ratio in grey scale (from 3×10^{-3} to $5 \times 10^{-3} \text{ kg kg}^{-1}$ in light grey and from 5×10^{-3} to $7 \times 10^{-3} \text{ kg kg}^{-1}$ in dark grey) from the Met Office analysis. The anomalies associated with *Irene* are a positive PV tower (4), a moisture anomaly (6), an upper-level negative PV anomaly depicted as a tropopause lift (5) and a surface potential-temperature anomaly (7). The anomalies associated with the extratropical environment are a baroclinic zone (1), diabatically-generated PV along the baroclinic zone (2) and an upper-level positive PV anomaly (3).

TRANSITION EXTRA-TROPICALE (5)

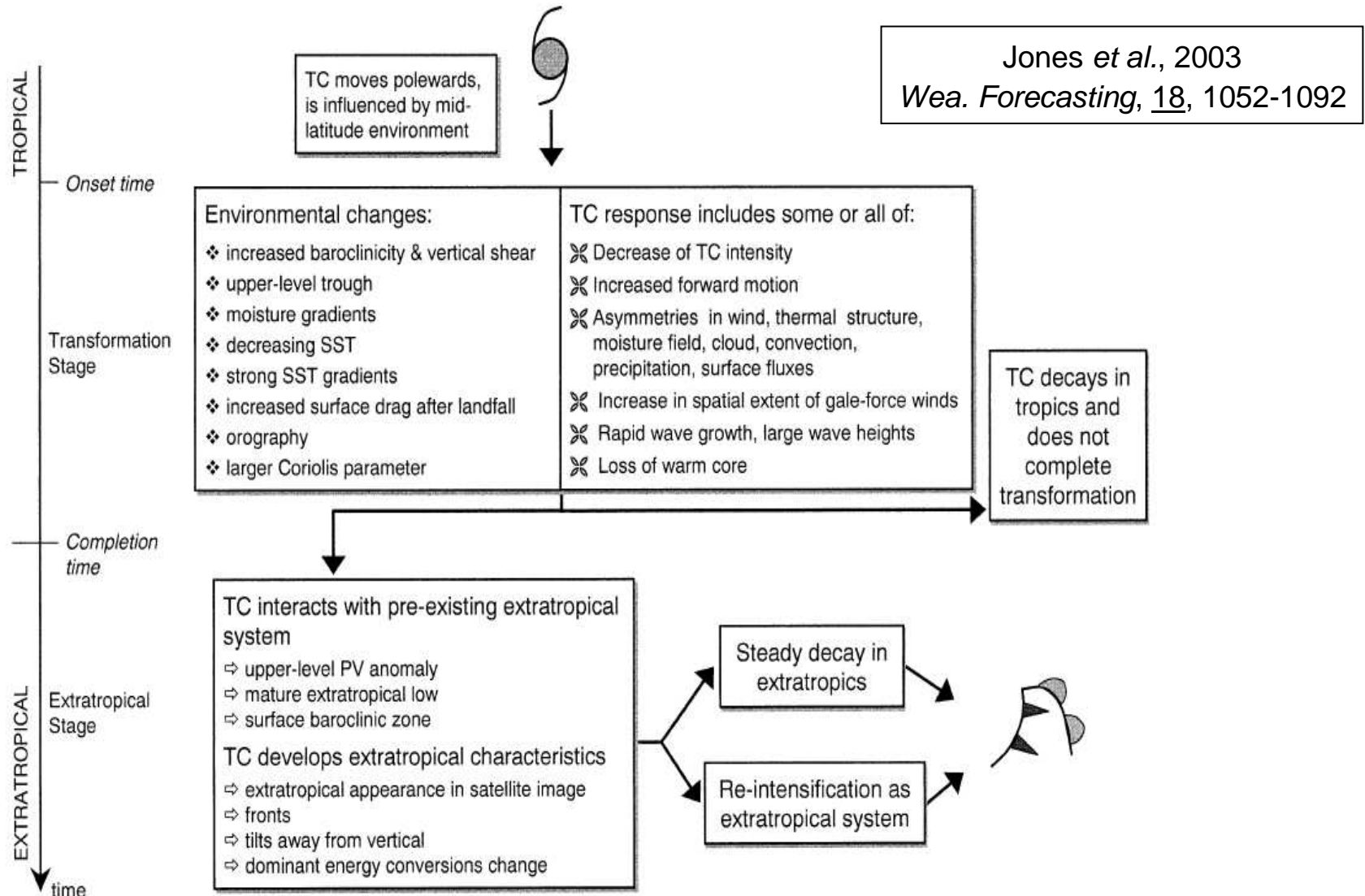
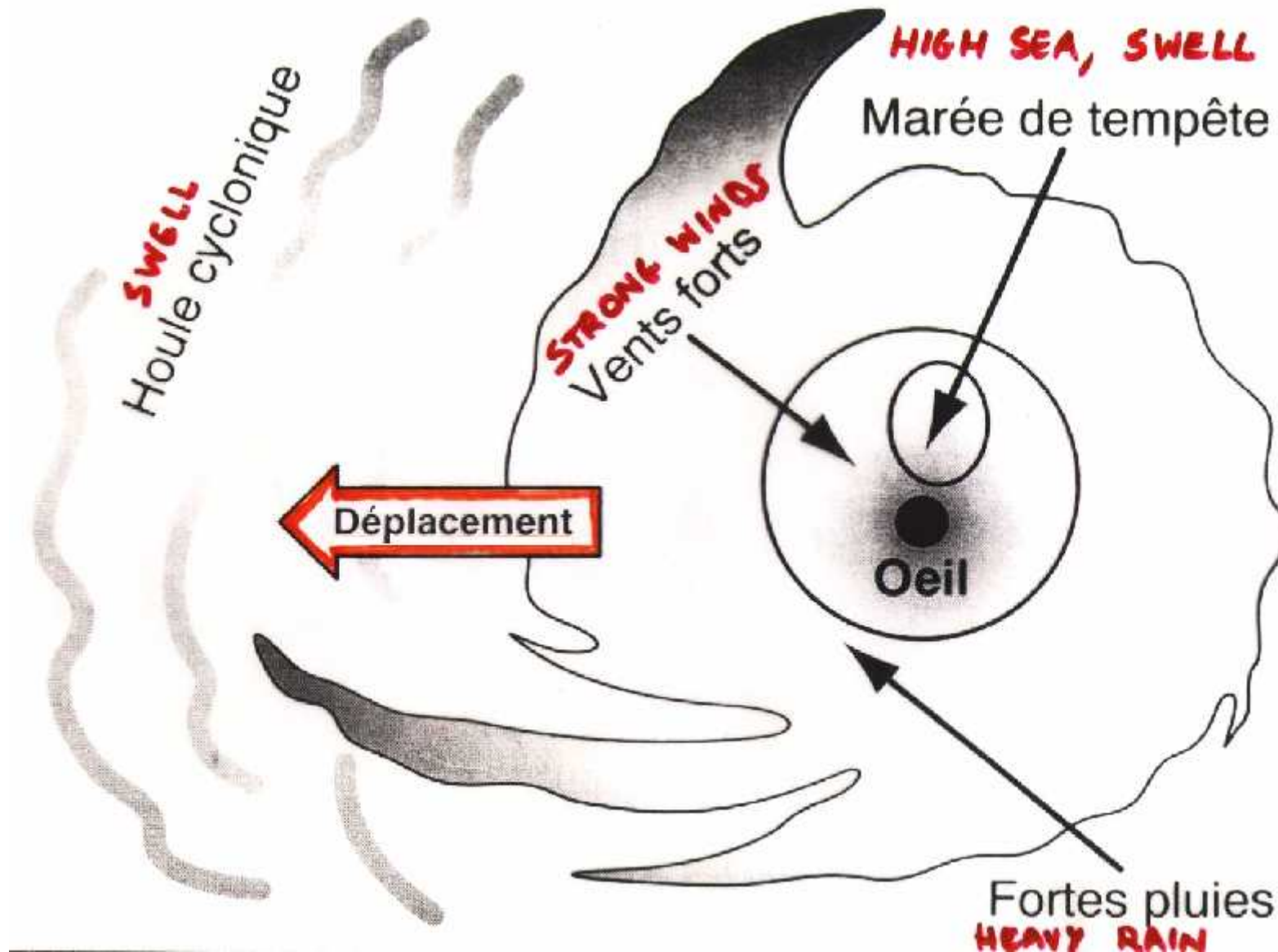
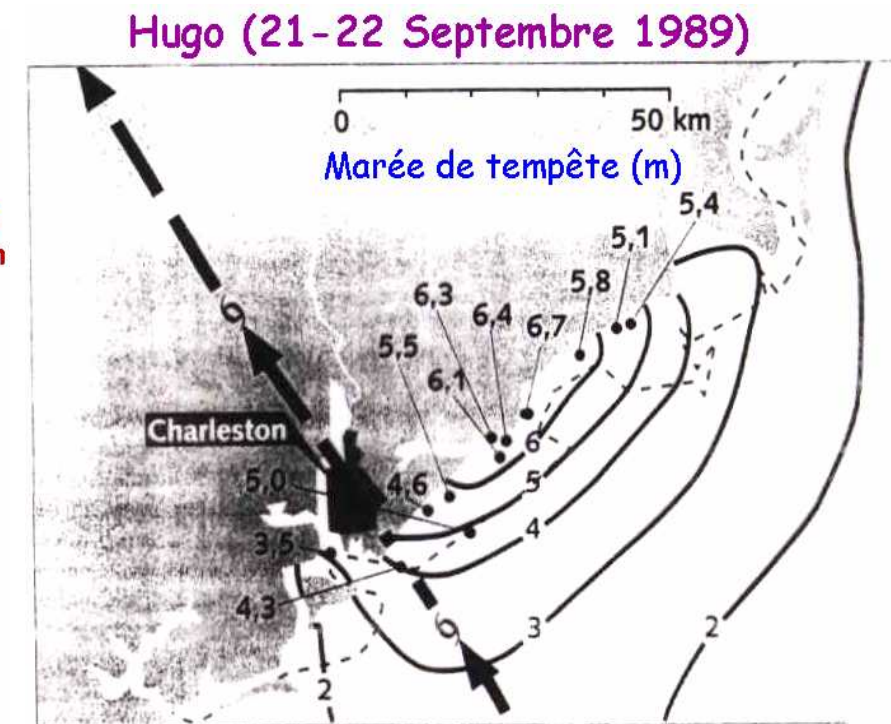
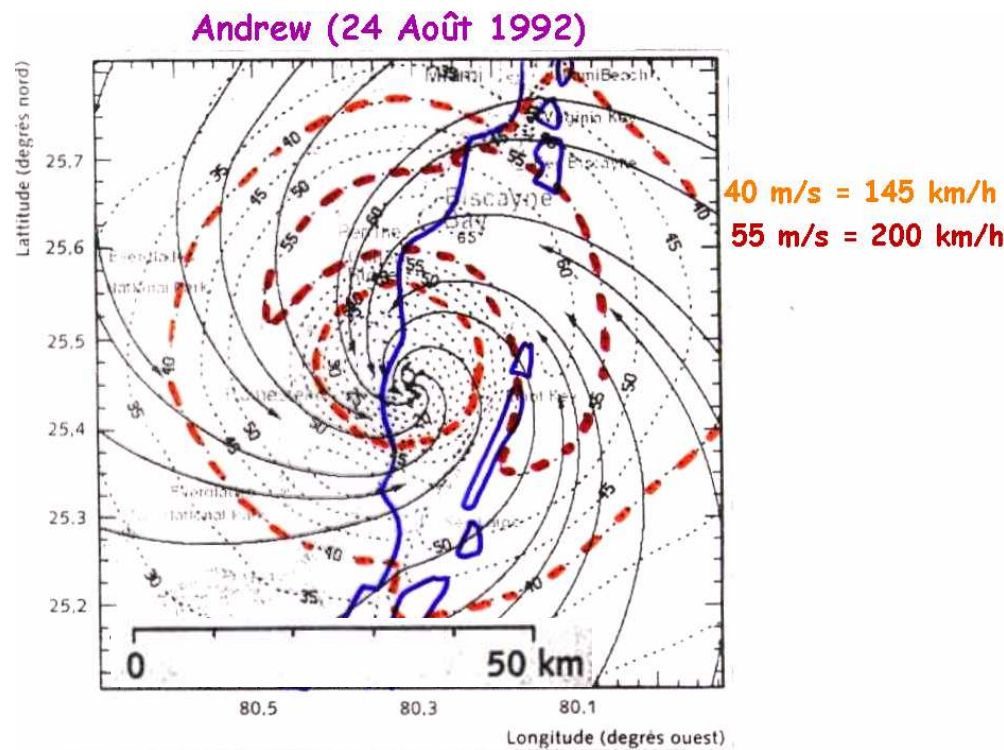


FIG. 11. A two-stage classification of extratropical transition based on the classification of Klein et al. (2000). The onset and completion times correspond to the definitions of Evans and Hart (2003). The “tropical” and “extratropical” labels indicate approximately how the system would be regarded by an operational forecast center.

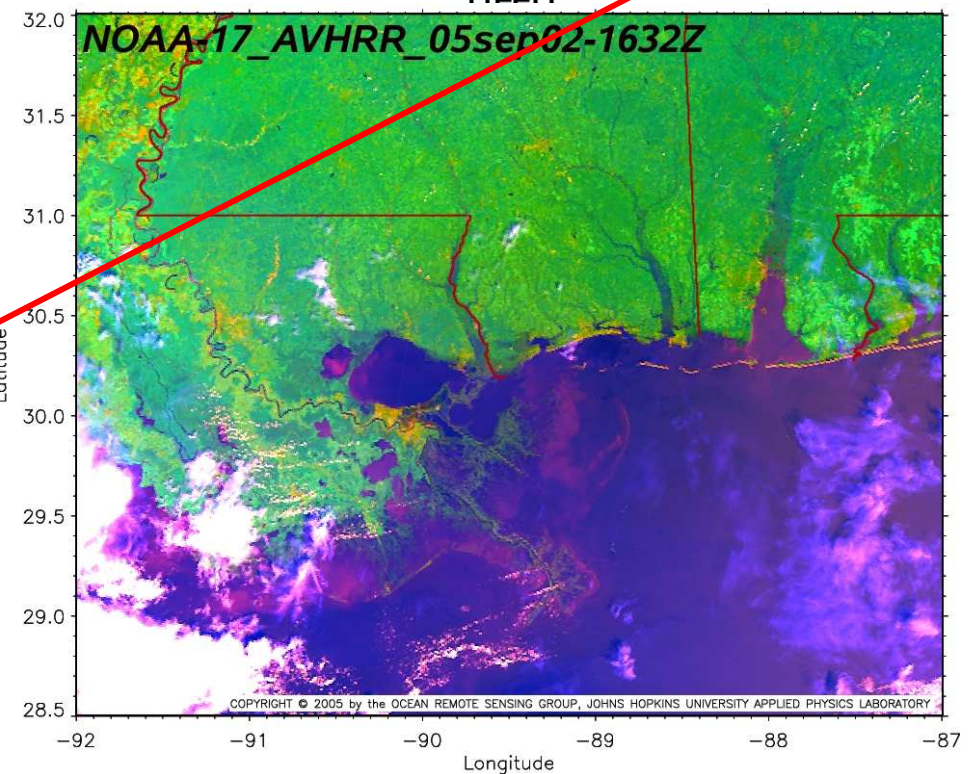
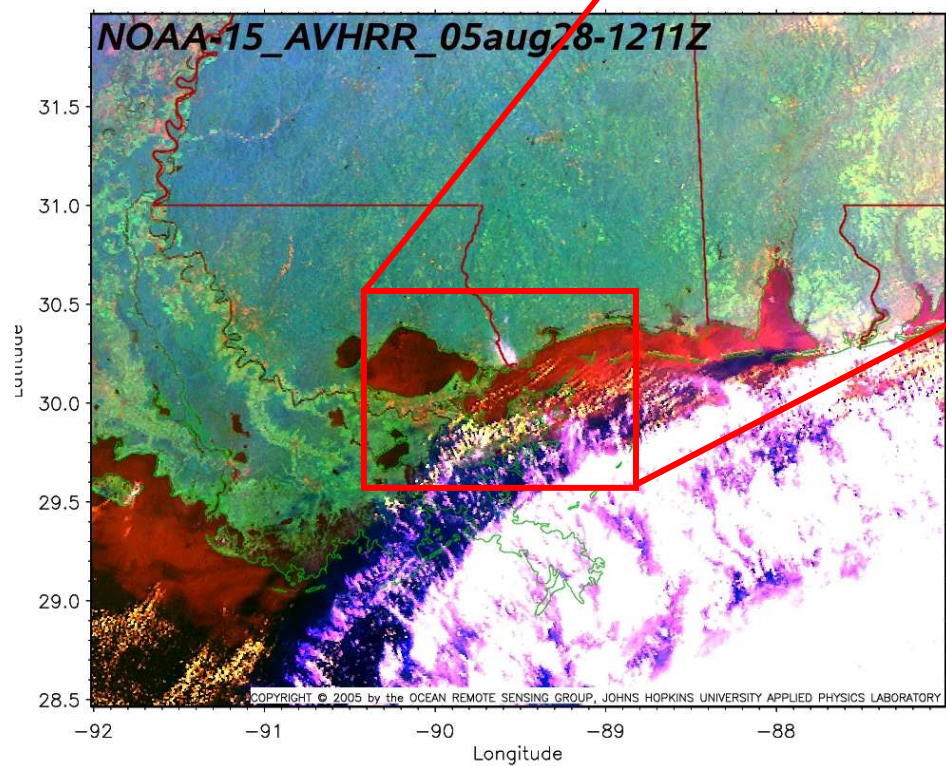
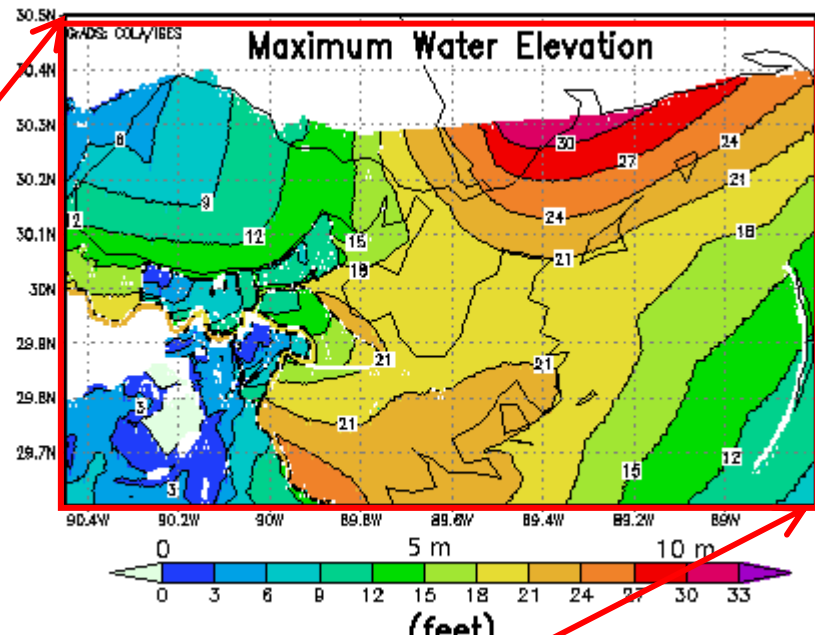
LES RISQUES LIES AUX CYCLONES (1)



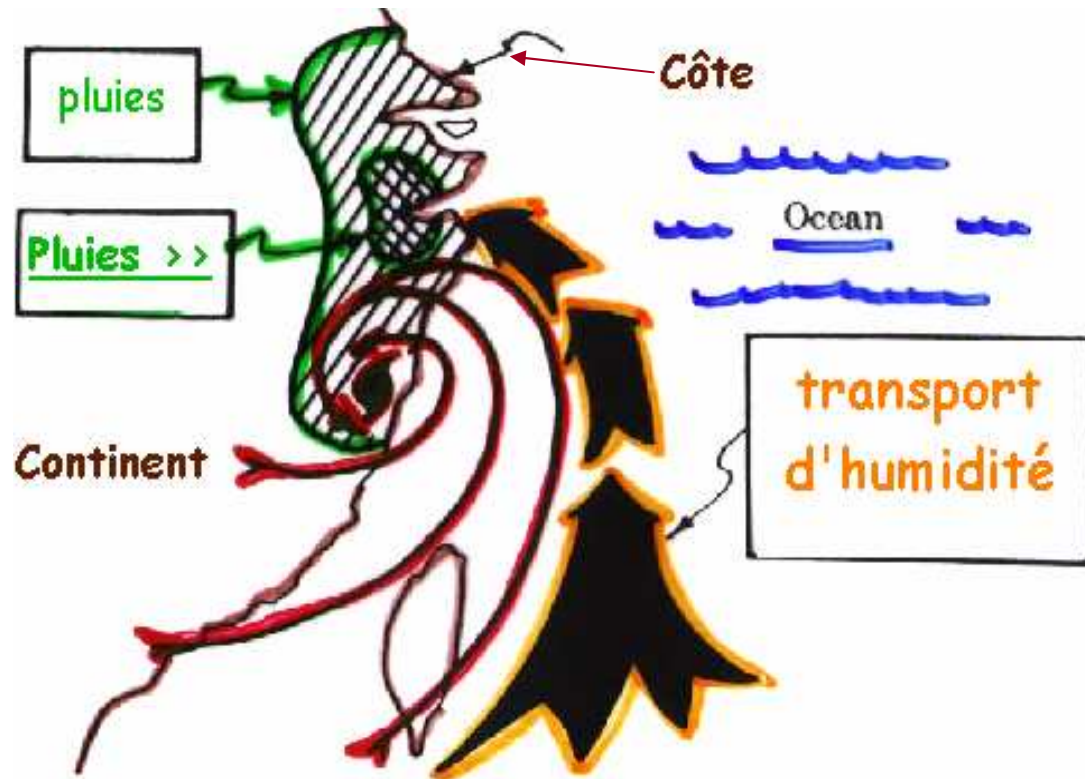
LES RISQUES LIES AUX CYCLONES (2)



Katrina 29 Août 2005 :
vents > 300 km/h, marée > 12 m



LES RISQUES LIES AUX CYCLONES (3)



Mitch
(Oct. 1998)

